Impact of PEGylation on antibody-loaded nanoparticulate drug delivery system on treatment of inflammatory bowel disease

Neha Shrestha [a,*], Yining Xu [a], Julien R. C. Prévost [b], Fiona McCartney [c], David Brayden [c], Raphaël Frédérick [b], Ana Beloqui [a], Véronique Préat [a,*]

[a]Advanced Drug Delivery and Biomaterials, Louvain Drug Research Institute, Université catholique de Louvain, 1200 Brussels, Belgium

[b]Medicinal Chemistry, Louvain Drug Research Institute, Université catholique de Louvain, 1200 Brussels, Belgium

[c] UCD School of Veterinary Medicine and UCD Conway Institute, University College Dublin, Belfield, Dublin 4, Ireland

*Corresponding authors

Véronique Préat
Advanced Drug Delivery and Biomaterials
Louvain Drug Research Institute
Université catholique de Louvain,
1200 Belgium
veronique.preat@uclouvain.be
+32 2 764 73 09

Neha Shrestha
Advanced Drug Delivery and Biomaterials
Louvain Drug Research Institute
Université catholique de Louvain,
1200 Belgium
shres.neha@gmail.com
+32473762961

Abstract

Nanoparticle-based oral drug delivery systems have the potential to target inflamed regions in the gastrointestinal tract by specifically accumulating at disrupted colonic epithelium. But, delivery of intact protein drugs at the targeted site is a major challenge due to the harsh gastrointestinal environment and the protective mucus layer. Biocompatible nanoparticles engineered to target the inflamed colonic tissue and efficiently penetrate the mucosal layer can provide a promising approach for orally delivering monoclonal antibodies to treat inflammatory bowel disease. The study aims to develop mucus-penetrating nanoparticles composed of poly(lactic-co-glycolic acid, PLGA) polymers with two different polyethylene glycol (PEG) chain lengths (2 kDa and 5kDa) to encapsulate monoclonal antibody against tumor necrosis factor-α (TNF-α). The impact of different PEG chain lengths on the efficacy of the nanosystems was evaluated *in vitro, ex vivo,* and *in vivo*. Both PLGA-PEG2k and PLGA-PEG5k nanoparticles successfully encapsulated the antibody and significantly reduced TNF-α secretion from activated macrophages and intestinal epithelial cells. However, only antibody-loaded PLGA-PEG2k nanoparticles were able to alleviate the experimental acute colitis in mice demonstrated by improved colon weight/length ratio, histological score, and reduced tissue-associated myeloperoxidase activity and expression of proinflammatory cytokine TNF-α levels compared with the control group. The results suggest that despite having no significant differences in the *in vitro* cell-based assays, PEG chain length has a significant impact on the *in vivo* performance of the mucus penetrating nanoparticles. Overall, PLGA-PEG2k nanoparticles were presented as a promising oral delivery system for targeted antibody delivery to treat inflammatory bowel disease.

Keywords: Mucus penetrating, PEGylated PLGA nanoparticles, antibody, inflammatory bowel disease, oral drug delivery

1. Introduction

Inflammatory bowel disease (IBD) is a relapsing chronic inflammatory disorder of the gastrointestinal (GI) tract. Ulcerative colitis and Crohn's disease are the two variants of IBD, with inflamed lesions which are colon-specific or widespread, respectively. IBD is a highly prevalent GI disease, with 6.8 million cases worldwide and increasing [1]. Conventional therapeutic options for IBD, such as aminosalicylates, corticosteroids, thiopurines, mainly provide symptomatic relief [2]. However, with increased knowledge and understanding of the underlying pathology of IBD, the role of the pro-inflammatory cytokine, TNF-α, in orchestrating the inflammatory process has been recognized [3]. Researchers have also demonstrated effective control of the IBD by blocking these inflammatory pathways [4-6]. Thus, systemic administration of antibodies against TNF-α (anti-TNF-α Ab), such as infliximab and adalimumab, has been established as a treatment approach for severe ulcerative colitis [7]. Owing to the chronicity of disease, repeated intravenous administration of the antibody is needed, which is linked with high cost, lower adherence rate, and systemic exposure-related life-threatening complications [8-10]. Most of these complications could be resolved by developing an orally delivered system that could deliver the anti-TNF-α antibody locally to the disease site.

Oral drug delivery systems are relatively cheaper and have higher patient compliance compared to injectables [11]. Furthermore, they can be exploited to locally deliver the antibody and maintain therapeutic concentrations in the inflamed regions whilst reducing systemic exposure. Among several oral delivery strategies, nanoparticle-based drug delivery systems are a promising approach to improve the efficacy of therapeutics at lower drug concentrations by enhancing the targeted interaction and uptake by inflamed regions in the colon. Furthermore, the preferential accumulation of nanosized particles in the inflamed sites of the GI tract due to pathophysiological changes (enzyme up-regulation, mucus layer depletion, accumulation of positively charged proteins) has already been demonstrated in previous studies [12-15]. Among several alternatives, nanoparticles based on biocompatible and biodegradable polymer poly(lactic-co-glycolic-acid) (PLGA) have demonstrated advantages over other systems by accumulating at the leaky regions of the inflamed intestine, thereby significantly extending

their residence time [16]. PLGA based nanoparticles has shown to successfully encapsulate and release peptides and proteins [17, 18].

Additionally, the nature of particle surface also plays a key role in its fate after oral administration. The colloidal stability of the nanoparticles after oral administration is a crucial factor for the successful delivery of encapsulated payload at the targeted site. The use of poly(ethylene glycol) (PEG) to modify the surface of nanoparticles imparts hydrophilicity to the surface thus reducing its interaction with the intestinal luminal content, enabling unobstructed passage to the targeted site [19, 20]. The hydrophilic PEG further confers a mucus-inert property to nanoparticles, resulting in diminished interaction with the mucus layer and enhancing the translocation through the mucus to the mucosa [11, 21]. Furthermore, the beneficial impact of the PEGylated surface on the attachment of nanoparticles to leaky inflamed intestinal regions has also been demonstrated, along with the capacity to translocate across the epithelium [22]. Thus, in this study, PEGylated PLGA nanoparticles were selected as a drug delivery vehicle for oral delivery of anti-TNF-α Ab to the inflamed colon. However, despite the impact of PEGylation on the efficacy of the oral nanosystems, the influence of PEG densities on antibody encapsulation and its efficacy in preclinical colitis models has not been studied yet.

Herein, we developed PLGA-PEG nanoparticles with two different PEG chain lengths for oral delivery of anti-TNF-α antibody (mAb). We evaluated the influence of two different PEGs on the efficacy of PLGA-PEG nanoparticles as oral anti-TNF-α antibody delivery systems. For this, PLGA-PEG polymer with PEG chain lengths, 2 kDa and 5kDa, were selected (PLGA-PEG2k and PLGA-PEG5k). The nanoparticles were characterized *in vitro* based on size, surface charge, stability, and antibody encapsulation, and release behavior. The cellular compatibility and the cellular interactions of the nanoparticles were evaluated with the intestinal cell line, Caco-2. The anti-inflammatory effect of these nanoparticles was also studied in lipopolysaccharide (LPS)-stimulated macrophages and intestinal cell models. *In vivo* oral efficacies of the nanoparticles were also studied in acute and chronic colitis models by studying the clinical activity, colon histological analysis, and quantification of neutrophil infiltration and local cytokines. Finally, the interaction of the nanoparticles with inflamed colonic tissues was also evaluated in an *ex vivo* model.

2. Experimental

2.1. Materials and cell lines

The materials used in this study are given in detail in Supplementary information S1.

The cell lines and culturing techniques used are also detailed in Supplementary information S2.

2.2. Preparation of nanoparticles

mAb-loaded PLGA-PEG2k (mAb-PLGA-PEG2k) and PLGA-PEG5k (mAb-PLGA-PEG5k) nanoparticles were prepared using a modified double emulsion technique [17, 23]. Briefly, the oil phase comprised of 50 mg of PLGA-PEG2k or PLGA-PEG5k dissolved in 0.5 mL of dichloromethane (DCM). The mAb solution (100 µL, ca. 20 mg/ml in buffer) was added to the oil phased and then homogenized using probe sonication (Branson Digital Sonifier, CT, USA) for 60 s using an ultrasound burst of 15 s followed by a 15 s pause at 30% amplitude to form a primary water-in-oil emulsion. Then the primary emulsion was added to 4 ml of emulsifier solution (0.5% sodium cholate solution, w/v), and was immediately homogenized using probe sonication for 2 min using an ultrasound burst of 15 s followed by a 15 s pause (30% amplitude). The finally formed w/o/w emulsion was then added to 12 mL of the emulsifier solution and stirred at room temperature for 90 min, to allow the evaporation of residual solvents. Thus, formed nanoparticles were washed twice with water using ultracentrifugation (27,216 x g, 30 min, 4°C) (Avanti® J-E, Beckman Coulter, USA). Finally, nanoparticles were suspended in Milli-Q water at a concentration of 10 mg/mL and stored at 4 °C until further use. Human mAb was used for all the experiments, except for *in vivo* studies where murine mAb was used instead. The same protocol was used for both the antibodies.

Empty nanoparticles were prepared using water, instead of drug solution, and using the same protocol as above. For the preparation of fluorescently labeled nanoparticles, 3,3'-Dioctadecyloxacarbocyanine Perchlorate (DiO) was used as the lipophilic dye. DiO solution was prepared by dissolving in dichloromethane (1 mg/mL, w/v). 100 µL of DiO solution was added to the PLGA-PEG solution in DCM. Then, the same protocol, as mentioned above, was used to prepare the fluorescently labeled

nanoparticles. The DiO-labelled nanoparticles (DiO-PLGA-PEG2k and DiO-PLGA-PEG5k) were used freshly after preparation.

2.3. *In vitro* Characterization of nanoparticles

Size and charge

The nanoparticles were characterized based on their physicochemical properties, such as size (hydrodynamic diameter, *z*-ave, and polydispersity index, PdI), and surface charge (zeta potential, ζ-potential). The size and PdI were measured using the dynamic light scattering technique, and the ζ-potential was measured using Laser Doppler Velocimetry. Both of the characteristics were measured using Malvern Zetasizer Nano (Malvern Instruments Ltd., United Kingdom). Before measurement, 100 µL of the nanoparticle dispersion was suspended in 900 µL of 10mM NaCl solution.

Stability study

The storage stability of the nanoparticles was evaluated at 4°C for 28 days. The size and charge of nanoparticles were measured using the abovementioned protocol at different points.

The stability of the empty PLGA-PEG nanoparticles was also studied in simulated GI fluids: simulated gastric fluid (SGF), fasted state simulated intestinal fluid (FaSSIF), and fed state simulated intestinal fluid (FeSSIF). A detailed description of the simulated fluids is given in Supplementary Information S3. The stability of PLGA-PEG nanoparticles was studied in gastric and intestinal conditions for 2 h and 6 h, respectively. 2.5 mg of nanoparticles were dispersed in pre-heated simulated GI fluids and incubated at 37 °C under moderate shaking. During the test period, 200 µL samples were withdrawn and dispersed in 800 µL of 10 mM NaCl solution, and size was measured using the dynamic light scattering technique. After each sample collection, the withdrawn volume was replaced with the respective pre-heated simulated fluids.

Drug encapsulation and release

mAb loaded PLGA-PEG nanoparticles (mAb-PLGA-PEG) were also studied based on the encapsulation efficiency (%, w/w) and loading degree (%, w/w), which were calculated using equations as shown in Supplementary information S4. The unencapsulated antibody was separated from the

nanoparticles using ultracentrifugation (24,000 *g* for 30 min at 4 °C) (Avanti® J-E ultracentrifuge (Beckman Coulter, USA). The antibody concentration was quantified using high-performance liquid chromatography (HPLC). The HPLC quantification method used is described in detail in Supplementary information S5.

The drug release was performed by suspending mAb loaded PLGA-PEG nanoparticles in SGF (without pepsin) and FaSSIF, for 2 h and 6 h respectively. The mAb-PLGA-PEG2k and mAb-PLGA-PEG5k nanoparticles were dispersed in 5 mL of SGF or FaSSIF and incubated at 37 °C with mild stirring (100 rpm). 750 µL of samples were collected at predetermined time intervals and replaced with prewarmed fresh release media. The collected aliquots were centrifuged (17,860 *g* for 10 min, 4 °C) and the supernatant was analyzed using HLPC to quantify the antibody released from the nanoparticles (see Supplementary information S5).

2.4. PEG quantification

The total and surface PEG were quantified using ^{1}H NMR using a Bruker 400 REM instrument, using a method as described elsewhere [23]. Briefly, the ^{1}H NMR spectra were recorded at 400 MHz with relaxation time set at 10 s and ZG at 90°, and the number of scans set to 8. PLGA-PEG nanoparticles were prepared using the previously mentioned method, but with deuterated solvents. To measure the surface PEG content, 3-(trimethylsilyl)-1-propanesulfonic acid, sodium salt (1 wt.-%) was used as an internal standard. A standard calibration curve was prepared for PEG2k and PEG5k homopolymer, with 1% 3-(trimethylsilyl)-1-propanesulfonic acid, sodium salt, and deuterated water (D20), which was used to quantify the PEG content on the surface of the nanoparticles. The actual mass of the nanoparticles was determined by weighing lyophilized nanoparticles. The total PEG content was determined by dissolving the lyophilized nanoparticles in Deuterated chloroform (CDCL3), with hexadeuterodimethyl sulfoxide (1 wt.-%, TMS) as an internal standard. A standard calibration curve was prepared for PEG2k and PEG5k homopolymer, with 1% TMS in CDCL3, which was used to quantify the total PEG content in the nanoparticles. The surface and total PEG content were calculated using the equation described in Supplementary information S6.

2.5. *In vitro* nanoparticle stability in mucin

PLGA-PEG2k and PLGA-PEG5k nanoparticles (5 mg/mL) were dispersed in 10 mg/ml mucin (porcine mucin, Sigma Aldrich, USA) and incubated at 37 °C under gentle agitation. Mucin solution was prepared by dissolving mucin powder in water overnight, and then centrifuged at 1, 000 x *g* to remove undissolved mucin fibers. The actual mucin concentration was determined by lyophilizing the mucin solution and weighing the resultant solid. Samples were collected at predetermined time points, and the size of the nanoparticles was measured using the dynamic light scattering technique (Malvern Zetasizer Nano ZS, Worcestershire, U.K.). Measurements were performed in triplicate at room temperature.

2.6. *In vitro* cell-based studies

Cellular viability study

The cellular toxicity of the PLGA-PEG2k and PLGA-PEG5k nanoparticles was tested on intestinal cells (Caco-2) and macrophages (J774) using a colorimetric assay with 3-(4,5-dimethylthiazol-2-yl)-(2,5-diphenyltetrazolium bromide) (MTT) [24]. Briefly, 20,000 cells (100 µL of 2 x 10^5 cells/mL) were seeded individually in each well in a 96 well plate (Nunc, Denmark), which were incubated overnight to allow the cells to attach to the well surface. The cells were washed once with pre-warmed HBSS buffer (prewarmed to 37 °C). To each well, 100 µL of different concentrations of nanoparticles (0.01 – 5 mg/mL) dispersed in a complete growth medium were added. The nanoparticles were incubated with cells for 4 h at 37 °C. After incubation, the cells were washed twice with HBSS buffer, and 0.5 mg/mL of MTT solution was added to each well and incubated for 3 h at 37 °C. After that, the excess MTT solution was removed and 200 µL of dimethylsulfoxide was added to dissolve the formed purple formazin crystal. The absorbance of the plate was read at 560 nm using a MultiSkan EX plate reader (Thermo Fisher Scientific, MA, USA). Cell culture media and 0.5% Triton X-100 were used as negative and positive controls, respectively. The negative controls were used to calculate the percentage of cellular viability.

Anti-inflammatory study

The *in vitro* anti-inflammatory activity of the empty and mAb-PLGA-PEG2k and mAb-PLGA-PEG5k were tested on J774 s and Caco-2 cell monolayers. The study allowed us to evaluate the ability of the antibody-loaded nanoparticles to inhibit the TNF-α secretion from cell lines exposed to inflammatory agents Murine antibody-loaded nanoparticles were used for evaluation in J774 monolayers, and human antibody loaded nanoparticles were used for study on Caco-2 monolayers. For J774 cells, 1 x 10^5 cells were seeded per well in each well in a 48-well plate and were allowed to attach overnight. The cells were then rinsed with pre-warmed HBSS solution and 300 µL of LPS (100 ng/mL) [24] in cell culture media were added to each well and incubated for 20 h. At the end of the incubation, 30 µL of nanoparticles (both empty and antibody-loaded) stock solution were added to LPS-treated cells to reach the final test concentrations (0.01 mg/mL, 0.1 mg/mL and 1 mg/mL). Nanoparticles were incubated with the cells for 4 h, and the supernatant from each well was collected. The supernatants were then centrifuged to remove any cell debris and then used to measure the TNF-α release, using an ELISA kit (eBioscience, Austria). The supernatant was also used to assess the cytotoxicity of these formulations on the stimulated cells using an LDH assay kit (Roche Diagnostics GmbH, Germany). The total protein content was also quantified by lysing the cells and using a bicinchoninic acid (BCA) assay. All the kits were used following the manufacturer's instructions. The results were expressed as the fold decrease in the TNF-α secretion compared to control (LPS-stimulated cells in the absence of formulations). Subsequently, based on the results obtained from the anti-inflammatory studies in the macrophages, antibody-loaded nanoparticles were also tested in Caco-2 cell monolayers. The detailed procedure of developing Caco-2 cell monolayers is given in Supplementary information S7. LPS and interleukin-1β were used to induce inflammation in the Caco-2 cell monolayer [25]. The cell monolayers were washed with pre-warmed HBSS buffer, and then 500 µL culture media supplemented with LPS (10µg/mL) and IL-1β (25 ng/mL) were added to the apical chamber of the cell monolayer and incubated for 20 h at 37° C. Then, mAb-PLGA-PEG2k and mAb-PLGA-PEG5k nanoparticles (final mAb concentration of 1 mg/mL) were added to cells and incubated for a further 4 h. The supernatants were collected and used to perform an LDH assay to assess cytotoxicity. The cell monolayers were then washed with pre-warmed HBSS buffer, and they were lysed using three freeze-thaw cycles. The intracellular TNF-α

content was quantified using ELISA (Invitrogen, USA). The total protein content was measured using a BCA kit (Pierce™ BCA Protein Assay Kit, Thermo Fisher Scientific). The kits were used as per the instructions from the manufacturer.

Cellular interaction study

The interaction of fluorescently-labeled PLGA-PEG2k and PLGA-PEG5k nanoparticles were evaluated with Caco-2 cells. Both qualitative and quantitative approaches were undertaken to assess the cellular interactions [26]. The cellular interaction was quantitatively studied with flow cytometry, and confocal microscopy was used for qualitative analysis. For the quantitative study, 500 µL of 1 x 10^6 cells/mL were seeded in a 24 well plate for 24 h. Then, the cells were washed twice with HBSS, and 500 µL of PLGA-PEG2k or PLGA-PEG5k nanoparticles (1 mg/mL) were added to the cells and incubated for 4 h at 37 °C. After the incubation period, the cells were washed twice with HBSS buffer, and the cells were detached using a trypsin-EDTA solution. The detached cells were washed once with HBSS buffer and were dispersed in 400 µL of phosphate buffer saline and analyzed using BD FACSVerse™ flow cytometer (BD Bioscience, USA). For each sample, 10,000 events were recorded and the results were analyzed using the FlowJo analysis software package (TreeStar, USA).

A confocal microscope (Zeiss™ confocal microscope, LSM 150, Zeiss, Germany) was used to qualitatively observe the interaction of the DiO-labelled nanoparticles with the Caco-2 monolayers. Before the study, the cell monolayer was washed twice with pre-warmed HBSS buffer. Then, DiO-labelled nanoparticles (1 mg/mL) were added to each well and incubated for 4 h at 37 °C. After incubation, the cells were washed with HBSS buffer. The cell monolayers were fixed with 4% paraformaldehyde. The cell membranes were stained with rhodamine-phalloidin and the nuclei were DAPI-stained, before observation under the confocal microscope. The images were analyzed by the Zen software (Zeiss, Germany) to obtain *y-z*, *x-z*, and *x-y* views of the cells.

2.7. *In vivo* efficacy of antibody loaded nanoparticles

Murine mAb-loaded nanoparticles were studied in six weeks old C57BL/6 female mice (18–20 g; Janvier Laboratories, France). Both acute and chronic colitis models were used to study the *in vivo* efficacy of the PLGA-PEG2k and PLGA-PEG5k nanoparticles [27]. Animals were housed under standard approved conditions with an ad libitum supply of food and tap water. The protocols used in this study were approved by the Université catholique de Louvain animal committee (2014/UCL/MD/033). For the acute colitis model, the inflammation was induced by the administration of 3 % w/v dextran sulfate sodium (DSS) in drinking water for five consecutive days, and colitis was assessed on day 8 [28]. The chronic colitis model is explained in detail in Supplementary information S8. Briefly, the inflammation was induced by the administration of 2.5% dextran sulfate sodium (DSS) in drinking water in three cycles, and the colitis was finally assessed on day 50. The schematic representation of the acute study is shown in supplementary information S9. Four groups were created with 10 animals in each group, and were treated differently: (i) healthy mice, untreated control group; (ii) mice with colitis, DSS-treated control group; (iii) mAb-PLGA-PEG2k nanoparticles treated group (5 mg/kg of mAb), and (iv) antibody loaded mAb-PLGA-PEG5k nanoparticles treated group (5 mg/kg of mAb). The nanoparticles were administered via oral gavage (5 mg/kg of the nanoparticles, the concentration of nanoparticles used was 10 mg/mL), and for control groups, water was administered via the same method. The gavage was performed every day until day 7. The weights of the animals were assessed every day until the end of the experiment. On day 8, the animals were sacrificed, and colon tissue samples were collected for further analysis.

Clinical activity scoring

The clinical activity scoring was performed for each animal in a group using the method described elsewhere [29]. Weight loss, stool consistency, and rectal bleeding were used to calculate the score (0-4) [29].

Colon weight/length ratio

After the sacrifice of animals, the colons were excised, and the luminal contents were cleaned. The colon's length and weight were measured and weighed respectively, to calculate the colon weight/length ratio. This ratio is used as an indicator of the severity and degree of colitis inflammation [24, 30].

Myeloperoxidase (MPO) activity

MPO assay was performed to quantify the MPO activity in the colonic tissue, which correlates with the severity of inflammation. Colon specimen from each animal were snap-frozen in liquid nitrogen immediately after extraction and stored at -80 °C until further assessment. The tissue sections were placed in hexadecyltrimethylammonium bromide HTAB buffer (0.5% HTAB in 50 mM potassium phosphate buffer, pH 6) containing protease inhibitor cocktail and homogenized gently while on ice. The homogenate was centrifuged at 10,000 *g* for 15 min at 4 °C. The supernatants were collected and 21 µL were added to a 96-well plate in triplicates (Nunc, Denmark). To each well 200 µL of a 0.167 mg/mL, O-dianisidine solution and 500 ppm in hydrogen peroxide in 50 mM phosphate buffer was added. The plate was then read at 460 nm for 60 min using a spectrophotometer (Spectrophotometer Spectramax M2e & program SoftMax Pro, USA) to determine the MPO activity. The total protein content was also analyzed using BCA analysis (Pierce™ BCA Protein Assay Kit, Thermo Fisher Scientific). The results were expressed as MPO units per g of protein, and each unit of MPO activity was defined as the amount equivalent that degrades 1 mmol/min of hydrogen peroxide at 25 °C [24].

Tissue cytokine quantification

The concentration of pro-inflammatory cytokine, TNF-α, in the colonic tissue was quantified using an ELISA kit (Invitrogen, USA). Colon homogenates were prepared from the snap-frozen colonic tissue samples using extraction buffer comprising of PBS with 1% sodium dodecyl sulfate and 1 tablet of complete protease inhibitor cocktail per 10 mL of extraction buffer (Roche Diagnostics, Belgium). UltraTurrax (IKA T18 Basic, Germany) was used to prepare the homogenates. The homogenates were then centrifuged for 10,000 *g* for 15 min at 4 °C. The supernatants were collected and stored at -80 °C until further analysis. The TNF-α was quantified in supernatants using ELISA, based on the manufacturer's instructions. The total protein content of the supernatants was also analyzed using a BCA assay (Pierce™ BCA Protein Assay Kit, Thermo Fisher Scientific).

Histological assessment

The colon segments fixed overnight with 4% formalin solution were used for histological assessment. The fixed tissue sections were embedded in paraffin. Two sets of three sections (10 µm) were cut which were 150 µm apart. Hematoxylin-eosin staining was performed on the sections, and the histological scoring was performed in a blind manner [24]. The classification system comprised of five grades of inflammation (0-4): 0, no structural change; 1, inflammation visible; 2, leukocytes present in the lamina propria; 3, leukocytes present in the epithelium (3.1 < 5% crypts involved, 3.2 < 50% crypts involved, 3.3 > 50% crypts involved); and 4, visible crypt destruction. Each mouse was scored individually and blindly, and each score is a representation of several sections from each mouse.

2.8. *Ex vivo* interaction study

The interaction between DiO labeled nanoparticles and the mouse colon with acute colitis was also studied using the *ex vivo* Eppendorf chamber model [31, 32]. The Eppendorf chamber method is described in detail and demonstrated schematically in the Supplementary information S10. Briefly, the colonic tissues were collected from the acute colitis murine model. The acute model was developed as mentioned above, and the animals were sacrificed on day 6 to obtain the colonic tissue. The colonic tissues were immediately placed on the Eppendorf chamber (as described in the Supplementary information S10). Krebs-Henseleit (KH) buffer was used as the medium in both apical and basolateral chambers. The media in the basolateral chamber was continuously oxygenated using carbogen gas (95% oxygen and 5% carbon dioxide). 75 µL of DiO labeled nanoparticles (2 mg/mL) dispersed in KH buffer were added to the apical side of the chamber and incubated for 2 h at 37 °C. At the end of the incubation period, the colonic tissues were washed gently, and directly embedded in OCT media (Tissue-Tek, USA). Cryosections (10 µm) of embedded tissues were cut and stored at -80 °C until further use. The slides containing sections were thawed at room temperature for 5 min and rinsed with PBS twice. Then, the sections were fixed using formaldehyde 4% for 10 min at room temperature and consequently washed twice with PBS. Then, the tissue sections were stained using wheat germ agglutinin (10 µg/mL, for 10 min at 37 °C). The sections were then washed three times with PBS and then mounted using DAPI enriched mounting media (Vectashield) and a glass coverslip. The slides were allowed to dry

overnight in dark, and were observed with a confocal microscope ((Zeiss™ confocal microscope, LSM 150, Zeiss, Germany), and data were analyzed with the Zen 3.0 Blue software (Zeiss, Germany).

2.9. Statistical analysis

The experiments were performed three times, with at least three independent replicates in each experiment (N=3, n ≥ 9). The data are represented as mean ± standard error of mean (Mean ± SEM). The normality of the data was analyzed using the Shapiro-Wilk normality test, and a one-way analysis of variance (ANOVA) followed by Tukey's *post-hoc* test was used. For other analyses, student's t-test or Mann-Whitney tests were used. The level of significance was set at probabilities of * $p < 0.05$, ** $p < 0.01$, and *** $p < 0.001$. The data were treated and analyzed using GraphPad Prism 8 program (CA, USA).

3. Results

3.1. Preparation and characterization of the nanoparticles

PLGA-PEG nanoparticles with two different PEG chain lengths, 2 kDa and 5kDa (referred to as PLGA-PEG2k and PLGA-PEG5k) were prepared using the double emulsification method. Two different PEG molecular weights were used to compare the influence of different PEG lengths on their *in vitro*, *in vivo*, and *ex vivo* performance. Empty PLGA-PEG2k and PLGA-PEG5k nanoparticles demonstrated a diameter of 209 and 211 nm respectively. mAb-PLGA-PEG2k and mAb-PLGA-PEG5k nanoparticles demonstrated a significant increase in the size to 239 and 235 nm, respectively, compared to the corresponding empty nanoparticles (shown in Figure 1A). Both empty and mAb loaded nanoparticles were monodisperse as exhibited by the low polydispersity index (PdI) of < 0.2 (Figure 1B) [33]. PLGA-PEG2k nanoparticles demonstrated a negative surface charge (ζ-potential) of −13.0 ± 0.8 mV, whereas PLGA-PEG5k nanoparticles showed a near-neutral surface charge of -2.4 ± 0.2 mV. After mAb encapsulation, the surface charge of PLGA-PEG2k and PLGA-PEG5k nanoparticles were slightly changed to -10.5 ± 1.6 mV and -0.8 ± 0.6 mV, respectively. Both PLGA-PEG2k and PLGA-PEG5k

demonstrated similar encapsulation efficiency (approximately 70%) and drug loading (approximately 2%) for both human (Figure 1C) and murine mAb.

In addition, the stability of the nanoparticles was also assessed using dynamic light scattering. The colloidal stability of the nanoparticles was assessed by monitoring the changes in the size and the PdI. The storage stability study demonstrated that both nanoparticles were able to retain their size and PdI for at least 28 days when stored at 4 °C (data not shown). Furthermore, both PLGA-PEG2k and PLGA-PEG5k nanoparticles demonstrated stability in SGF and FaSSIF by retaining their size and PdI, as shown in Figure 1D and Supplementary information S11, respectively. However, when incubated in FeSSIF, the size of the PLGA-PEG2k and PLGA-PPEG5k nanoparticles decreased and the PdI increased. Furthermore, the destabilization effect in FeSSIF was observed to a higher extent in PLGA-PEG5k nanoparticles.

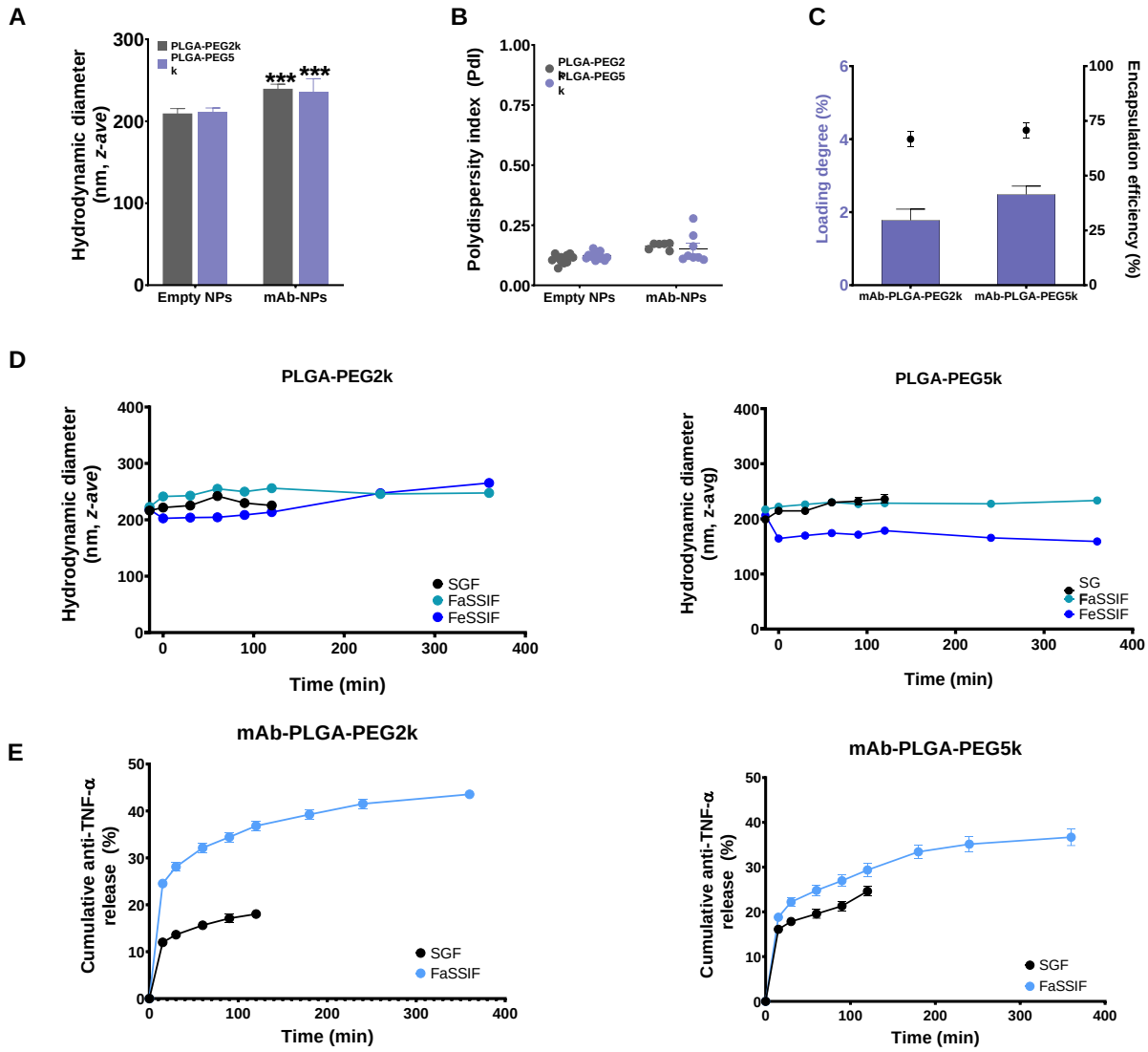

Figure 1 Physicochemical characterization of PLGA-PEG2k and PLGA-PEG5k nanoparticles. *(A) Size and (B) polydispersity index of empty PLGA-PEG2k and PLGA-PEG5k* nanoparticles (NPs) and mAb loaded (mAb-NPs), *determined using DLS technique. (C) Anti-TNF-α antibody encapsulation efficiency (%, dot plot) and loading degree (%, bar graph) in mAb-PLGA-PEG2k and mAb-PLGA-PEG5k nanoparticles. 9D) The in vitro stability study of PLGA-PEG2k and PLGA-PEG5k nanoparticles in simulated gastric fluid (SGF), Fasted state simulated intestinal fluid (FaSSIF), and fed state simulated intestinal fluid (FeSSIF). The size of the nanoparticles were measured using dynamic light scattering technique (E) The in vitro release profile of anti-TNF-α from PLGA-PEG2k and PLGA-PEG5k nanoparticles in*

simulated gastrointestinal fluid at 37 °C. Data is shown as mean ± SEM. (N=3, n=9). (p< 0.05, and *** p< 0.001)*

The *in vitro* release of the antibody from the nanoparticles was also evaluated SGF (without pepsin) and FaSSIF. To mimic the passage of the nanoparticles in the GIT, transit time of the stomach and intestine was considered and thus the release studies were performed for 2 h in SGF and 6 h in FaSSIF [26]. The release profile of mAb from PLGA-2k and PLGA-PEG5k nanoparticles in SGF and FaSSIF are shown in Figure 1E, respectively. A biphasic mAb release, with initial burst release followed by sustained release, was observed from both nanoparticles in both conditions. In acidic gastric condition, antibody was released in higher amounts (25%) from PLGA-PEG5k nanoparticles as compared to PLGA-PEG2k nanoparticles (18%) at the end of the 2 h incubation. However, there were no significant differences in the cumulative antibody released from both the nanoparticles in simulated intestinal fluid.

3.2. PEG quantification and *in vitro* mucin stability

The PEG content on the surface of the nanoparticles and in total was evaluated using the ^{1}H NMR method, as described elsewhere [23]. A calibration curve was prepared individually for quantifying the surface and total PEG content (shown in Supplementary information S6). As shown in Figure 2A, the total PEG content observed was 10% (w/w) and 22 % (w/w) for PLGA-PEG2k and PLGA-PEG5k nanoparticles, respectively. For both the nanoparticle types, it was observed that >90% of the PEG was present on the surface of the nanoparticles. After quantifying PEG content in the nanoparticles, the colloidal stability of these mucus-inert properties of PLGA-PEG nanoparticles was studied in mucin solution using dynamic light scattering. The stability of the nanoparticles was tested in mucin solution at 37°C for 3 h. As shown in Figures 2B and 2C, the particle size and particle size distribution did not change significantly during incubation in the mucin solution until 3 h.

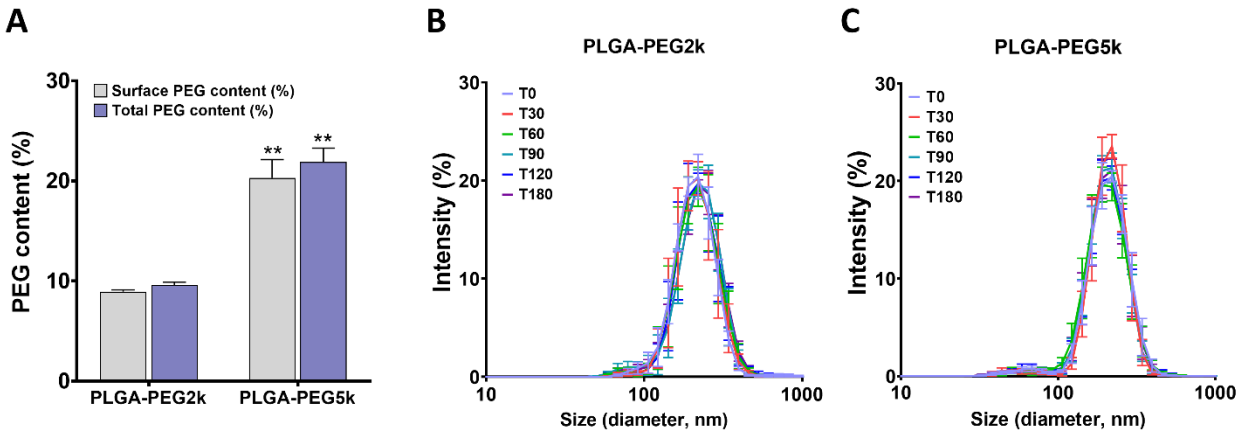

Figure 2. PEG quantification and in vitro mucin stability *(A) Total and surface PEG density determined using* ^{1}H *NMR. (B) In vitro mucin interaction. The size distribution of PLGA-PEG*2k *and PLGA-PEG*5k *nanoparticles after incubation with mucin solution for 3 h at 37 °C. Data is shown as mean ± SEM. (N=3) (** p< 0.01, PLGA-PEG*2k *vs PLGA-PEG*5k*).*

3.3. Cellular studies

Cellular viability studies

Before performing *in vitro* cell-based studies, the nanoparticles' influence on the viability of the tested cell lines was assessed. The cellular viability studies were performed on human colonic adenocarcinoma enterocytes (Caco-2) and murine macrophages (J774) using MTT assay. The presence of possible concentration-dependent and formulation-dependent toxicity was studied by incubating different concentrations of nanoparticles with both cell lines for 4 h. Both empty and mAb-loaded PLGA-PEG nanoparticles were evaluated for possible toxicity. In Caco-2 cells, a decrease in cellular viability was observed in a concentration-dependent manner (Figure 3A). A similar concentration-dependent trend was also observed when nanoparticles were exposed to the J774 cells (Figure 3B). Nonetheless, even at the highest tested concentration (5 mg/mL), all the nanoparticle variants demonstrated cellular viability of > 70% in both Caco-2 cells and J774 cells. Based on the cellular viability studies, the

concentration of nanoparticles with no or minimal cytotoxic effects was selected for further cell-based studies.

Anti-inflammatory studies in vitro

The anti-inflammatory activity of mAb-PLGA-PEG2k and mAb-PLGA-PEG5k nanoparticles was tested in LPS-stimulated J774 cells, and was compared to different controls: buffer-treated, empty nanoparticles, and mAb solution. The mAb solution showed a significant reduction in TNF-α secretion from the J774 cells compared to medium-treated cells (Figure 3C). Empty nanoparticles did not display any effect on the TNF-α levels, indicating that the nanoparticles themselves did not have any anti-inflammatory effect. However, for mAb-loaded nanoparticles, a concentration-dependent decrease in the secretion of the cytokine was observed. No significant differences between the anti-TNF-α-loaded PLGA-PEG2k and PLGA-PEG5k nanoparticles were detected. Based on these results, the nanoparticle concentration with the highest anti-inflammatory activity in stimulated J774 cells was selected to perform an anti-inflammatory activity study in LPS and IL-1β stimulated Caco-2 cell monolayers. In this study, culture media-treated cells were used as the control group (Figure 3D). Similar to J774 cells, both the antibody-loaded nanoparticles significantly reduced the pre-stimulated intracellular TNF-α content. Overall, this study demonstrated that the nanoparticles retained the biological activity of the encapsulated antibody following synthesis.

Cellular interaction study

In addition to understanding the biological activity of the encapsulated antibody, it is also important to evaluate the nanoparticle interactions at the cellular level. The interactions were analyzed qualitatively using confocal microscopy and quantitatively using flow cytometry. For both the studies, DiO-labelled PLGA-PEG2k and PLGA-PEG5k nanoparticles were used. The quantitative flow cytometry results (Figure 3E) demonstrated that both DiO-PLGA-PEG2k and DiO-PLGA-PEG5k nanoparticles interacted with the two intestinal cell lines, as observed with a significantly higher number of positive events and mean fluorescence intensity. As seen with previous studies, no differences were observed between the two PEG molecular weights. In the confocal fluorescence images (Figure 3F), DiO-labelled nanoparticles represent the green channel, the blue channel is indicative of the DAPI stained nuclei and

the red channel represents rhodamine-phalloidin stained cell membranes. Similar to quantitative analysis, the orthogonal confocal images demonstrate an interaction between nanoparticles with the cell monolayer. Both the DiO-PLGA-PEG2k and DiO-PLGA-PEG5k nanoparticles were found associated with the cell surface and were also observed in-between the cells and intracellularly.

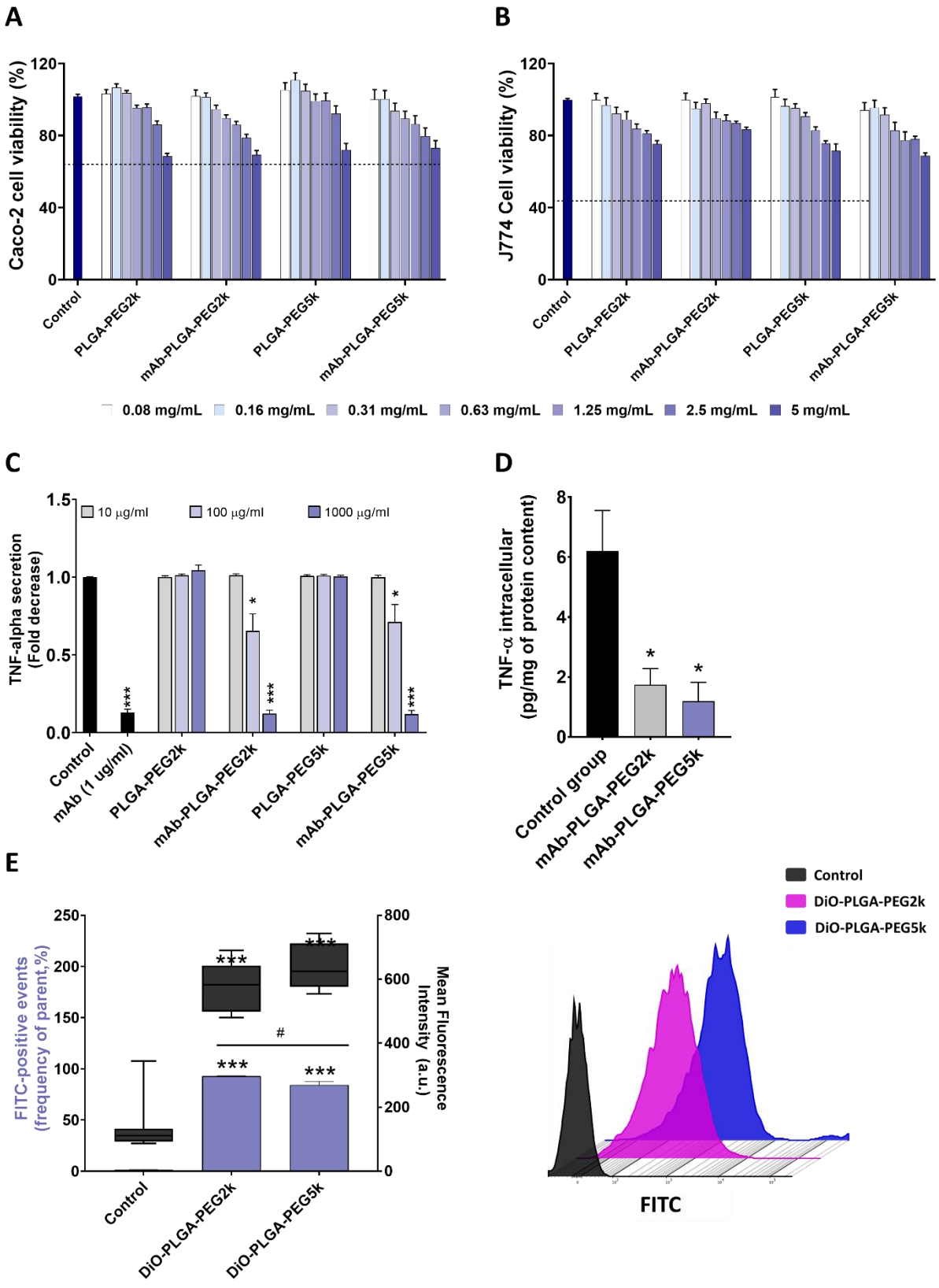
A
Caco-2 cell viability (%)
120
80
40
0
Control
PLGA-PEG2k
mAb-PLGA-PEG2k
PLGA-PEG5k
mAb-PLGA-PEG5k
B
J774 Cell viability (%)
120
80
40
0
Control
PLGA-PEG2k
mAb-PLGA-PEG2k
PLGA-PEG5k
mAb-PLGA-PEG5k
0.08 mg/mL
0.16 mg/mL
0.31 mg/mL
0.63 mg/mL
1.25 mg/mL
2.5 mg/mL
5 mg/mL
C
TNF-alpha secretion (Fold decrease)
1.5
1.0
0.5
0.0
10 μg/ml
100 μg/ml
1000 μg/ml
*
***
Control
mAb (1 ug/ml)
PLGA-PEG2k
mAb-PLGA-PEG2k
PLGA-PEG5k
mAb-PLGA-PEG5k
D
TNF-α intracellular (pg/mg of protein content)
8
6
4
2
0
*
*
Control group
mAb-PLGA-PEG2k
mAb-PLGA-PEG5k
E
FITC-positive events (frequency of parent,%)
250
200
150
100
50
0
Mean Fluorescence Intensity (a.u.)
800
600
400
200
0
***
***
***
#
Control
DiO-PLGA-PEG2k
DiO-PLGA-PEG5k
Control
DiO-PLGA-PEG2k
DiO-PLGA-PEG5k
FITC
F
Control
DiO-PLGA-PEG2k
DiO-PLGA-PEG5k

Figure 3. In vitro cell-based studies *Cellular viability study of (A) Caco-2 cells and (B) J774 cells using MTT assay. The cells were individually incubated with PLGA-PEG*2k *and PLGA-PEG*5k *nanoparticles, empty and antibody loaded, for 4 h at 37 °C. Evaluation of the anti-inflammatory properties PLGA-PEG nanoparticles on the inhibition of TNF-a secretion in LPS-stimulated (C) J774 macrophages and (D) Caco-2 cell monolayer, after co-incubation for 4 h at 37 ºC. Cell nanoparticles interaction study (E) Flow cytometry analysis of interaction of the DiO-labelled PLGA-PEG*2k *and PLGA-PEG*5k *nanoparticles with Caco-2 cells after co-incubation for 4 h at 37 °C. The frequency of positive events and mean fluorescence intensity are represented in the bar graph, and the flow cytometry graph is also shown. (F) Confocal images of DiO labelled nanoparticles interacting with Caco-2 cell monolayer after co-incubation for 4 h at 37 °C. Red channel represents the cell membrane stained with rhodamine-phalloidin, blue channel represents DAPI stained nuclei and the green channel represents the DiO labelled nanoparticles (Scale bar = 50 µm). Data shown as mean ± SEM (N=3, n=9) (* p< 0.05 and *** p< 0.001, as compared to untreated control group, (# p< 0.05, PLGA-PEG*2k *vs PLGA-PEG*5k*)*

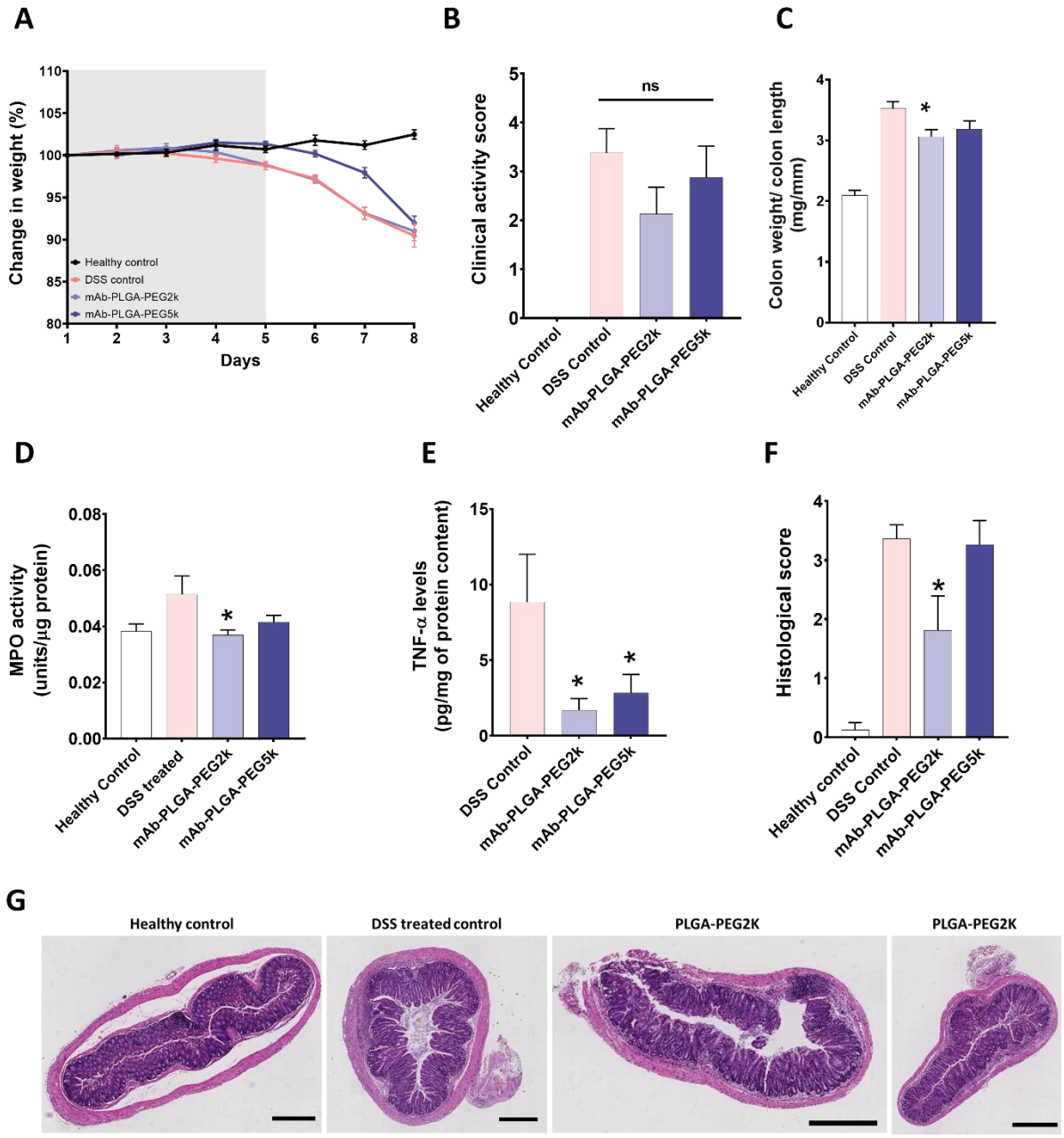

3.4. *In vivo* study in a murine colitis model

The influence of mAb-PLGA-PEG2k and mAb-PLGA-PEG5k nanoparticles was tested in both acute and chronic colitis models [27]. Both models were induced by administering DSS in drinking water in different schedules (as shown in Figure S8 and S9 in the supplementary file). The mice were evaluated based on the inflammatory clinical activity, colon structure and histology, MPO activity, and pro-inflammatory cytokine levels in colonic tissues [24, 30].

Inflammatory response

After the acute colitis experiment, the mice were sacrificed on day 8, and the animals were evaluated based on clinical activity scoring. The clinical activity scoring (on a scale of 0-4) was calculated considering the weight loss, stool consistency, and rectal bleeding, using the protocol by Melgar *et al* [29]. The results from the performance of the free antibody solution in acute colitis model is shown in detail in Supplementary file S12. The daily weight loss (%) of the mice during the acute colitis induction and treatment is shown in Figure 4A, and the clinical scoring on day 8 is shown in Figure 4B. Both clinical activity scores and the drastic weight loss observed in DSS-treated mice, as compared to the control mice groups demonstrate successful induction of acute colitis in all the DSS-tested groups.

The severity and extent of inflammation in the mice colon were assessed using the colon weight/colon length parameter of the excised colon [30, 34]. The observed colon weight/colon length ratio for all the tested groups is shown in Figure 4C. When compared to healthy mice, there is a significant increase in the ratio for all the DSS-treated groups, further indicating successful colitis induction. The mAb-PLGA-PEG nanoparticles were compared with the DSS control group. mAB-PLGA-PEG2k nanoparticles demonstrated a significant decrease (*p <0.05) in the colon weight/length ratio, as compared to the DSS control group, indicating its effectiveness as an anti-inflammatory system. However, despite showing a slight decrease in the ratio for mAb-PLGA-PEG5k treated groups, it was not significant compared to the DSS control group.

Figure 4. *In vivo efficacy study in DSS induced acute colitis murine model. The study included four groups (with eight mice in each group): (i) healthy mice, (ii) DSS treated control mice, (iii) PLGA-PEG*2k *treated DSS mice, and (iv) PLGA-PEG*5k *treated DSS mice. (A) Daily changes in body weight in DSS-induced acute colitis mice and in healthy mice (% respect to initial weight at day 1). (B) Clinical activity scoring of the four groups on the day of sacrifice (Day 8). (C) Colon weight/length ratio for all the tested groups. (D) MPO activity and (E) pro-cytokine TNF-α levels in colonic tissues on day 8 (F) Blind histological scoring of the colonic*

tissues of the groups and (G) Histological sections of the colon stained with hematoxylin-eosin. (Scale bar = 400 µm) Data shown as mean ± SEM (n=8) (p< 0.05, ** p< 0.01 as compared to DSS treated control group)*

MPO activity and cytokine quantification in colonic tissue

The colon tissue-associated MPO activity provides quantitative data on neutrophil infiltration which displays the severity of colitis [35]. The MPO activity in the excised colonic tissues of different groups on the day of sacrifice is shown in Figure 4D. Similar to the colon weight/length parameter, only the mAb-PLGA-PEG2k nanoparticles-treated group demonstrated a significant reduction in the colonic tissue associated MPO activity, compared to the DSS control group (*p < 0.05).

In addition, the colonic tissue associated level of pro-inflammatory cytokine (TNF-α) was also quantified, as an antibody against TNF-α is being delivered via the nanoparticles. Contrary to the MPO activity study where only the mAb-PLGA-PEG2k nanoparticles were efficacious, both types of antibody-loaded nanoparticles demonstrated a significant reduction in the level of TNF-α in the colonic tissue compared to the DSS control group. The decrease in the levels of TNF-α further confirms the effectiveness of the mAb-PLGA-PEG2k nanoparticles for orally delivering anti-TNF-α.

Histological analysis

The colonic tissues were evaluated for histological changes occurring due to inflammation. A blind histological scoring of the colonic tissues was performed on the H&E-stained tissue sections (as shown in Figure 4F, and in supplementary information Figure S13), which demonstrated a significant reduction in the inflammation for mAb-PLGA-PEG2k treated group, as compared to the DSS control group (*p < 0.05). The reduction in inflammation in the mAb-PLGA-PEG2k treated group was also observed in the hematoxylin-eosin-stained colon sections (Figure 4G). However, the PLGA-PEG5k nanoparticles treated group did not demonstrate any improvement in the inflammation, as observed in histological scoring. The results from the performance of the antibody-loaded nanoparticles in the chronic colitis model are given in detail in Supplementary file S14S.

3.5. *Ex vivo* interaction study

The interaction of the nanoparticles with inflamed colonic tissues was studied using an *ex vivo* Eppendorf chamber model (as shown in Supplementary information S10). DiO-labelled nanoparticles were used to study the interaction observed under a confocal microscope (as shown in Figure 5). In the image, the green channel represents DiO-labelled nanoparticles, the red channel represents wheat germ agglutinin (WGA) stained glycoconjugates and the blue channel represents the DAPI stained nuclei. The images demonstrate both DiO-PLGA-PEG2k and DiO-PLGA-PEG5k nanoparticles interact with the colonic tissues, however, it can be seen that the interactions are stronger for PLGA-PEG2k nanoparticles. The results corroborate with the findings in the *in vivo* efficacy study in the acute colitis model, where mAb-PLGA-PEG2k nanoparticles exhibited higher effectiveness towards diminishing inflammation in the colon.

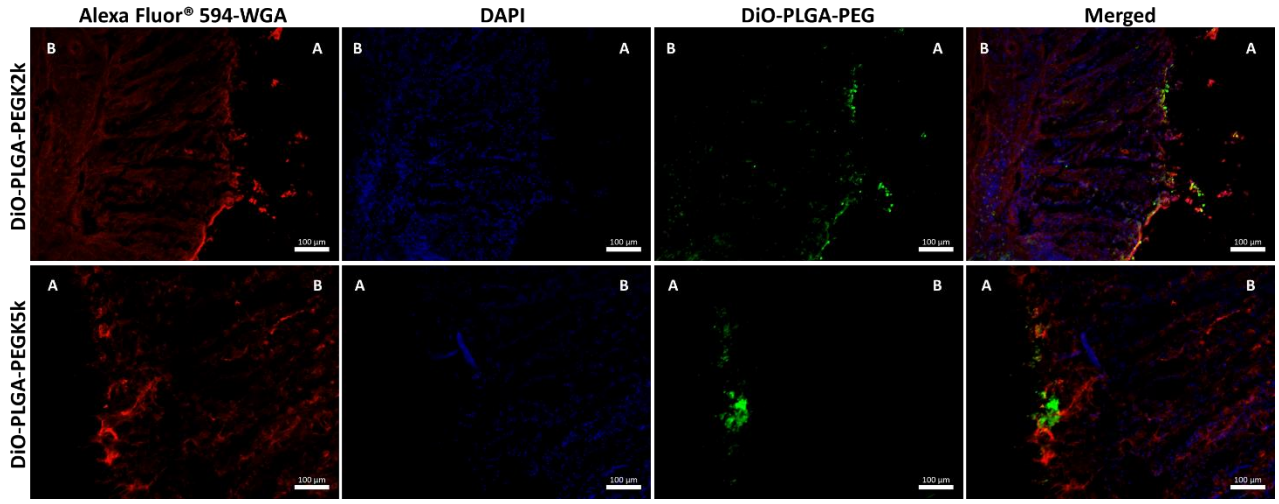

Figure 5. *Confocal images of DiO-PLGA-PEG2k and DiO-PLGA-PEG5k nanoparticles (green channel) interacting with colon from acute colitis murine model. (Red channel: Alexa fluor® 594 wheat germ agglutinin, Blue channel: DAPI stained nuclei) mounted in Eppendorf chamber ex vivo model. (Scale bars = 100 µm. A, apical side; B, basolateral side*

4. Discussion

The use of orally administered nanoparticles for localized delivery of active pharmaceutical ingredients (including biologics) at targeted inflamed regions of GIT has been extensively studied [11, 36, 37]. There are several potential benefits of using an oral anti-TNF-α mAb drug delivery system for treating IBD, including lower cost, improved patient adherence, easy administration, and low systemic exposure leading to reduced risks of life-threatening complications [8-10]. However, the efficiency of oral protein formulations for colon-targeted therapy is greatly diminished by several factors including premature release and degradation before reaching the inflamed colonic regions. Furthermore, the mucus barrier lining the GIT poses is another major barrier limiting the drug accumulation at the site of action. The different components of the mucus layer can entrap particulate-based drug delivery systems by forming multiple interactions (such as hydrophobic interactions, electrostatic interactions, polymer interpenetration) with the nanoparticle surface. Herein, PLGA-PEG-based nanoparticles were selected to encapsulate and locally deliver anti-TNF-α mAb, as it combines the targeted delivery potential of PLGA and mucus penetrating property of PEG. The developed systems were evaluated *in vitro* and *in vivo* to assess their potential for delivering anti-TNF-α mAb to treat IBD.

PEG modification of nanoparticles and drug delivery systems is used to improve stability, limit the interaction with biological contents and increase blood circulation time. Several studies have also demonstrated the influence of PEG content on imparting mucus-penetrating property to orally deliverable nanoparticles [23, 38, 39]. The interest in mucus-inert nanoparticles has significantly increased due to their ability to overcome one of the major barriers to intestinal absorption [19]. Thus, we compared PLGA-PEG nanoparticles with two different PEG chain lengths (PEG2k and PEG5k) in their ability to successfully encapsulate and deliver anti-TNF-α mAb. We observed that using PEG with higher molecular weight (PLGA-PEG5k) resulted in nanoparticles with near-neutral surface charge as compared with PLGA-PEG2k nanoparticles (−13 mV vs. −2 mV, respectively) [23]. In addition to characterization, understanding the stability of the nanoparticles in the GIT is of utmost importance, as any changes on the surface and physiochemical properties of the

nanoparticles can greatly alter the expected interaction at the target site. Gastrointestinal fluids are highly complex media, thus studying the stability of nanoparticles only in commonly used buffers will only yield limited information regarding the stability of the nanoparticles after oral administration [26]. Therefore, the stability of PLGA-PEG2k and PLGA-PEG5k nanoparticles were studied in simulated gastrointestinal fluids: SGF, FaSSIF, and FeSSIF. Both nanoparticles demonstrated good stability in SGF and FaSSIF, however, reduced stability was observed in FeSSIF. A possible explanation for the effect can be attributed to five-fold higher levels of bile salts, a natural solubilizing agent in FeSSIF (see supplementary information S3). The presence of a high amount of bile salts significantly accelerates the dissolution of the nanoparticles, thus resulting in a decrease in the size of the nanoparticles [40, 41]. Furthermore, the higher destabilization effect of PLGA-PEG5K in FeSSIF can be accredited to the higher hydrophilicity of PLGA-PEG5k nanoparticles, owing to its higher PEG content [42]. Considering the stability profile in simulated gastrointestinal fluid, it can be recommended to administer these nanoparticles in a fasted state to maintain their colloidal stability after administration. To fully establish the effectiveness of the formulation, it is critical to understand the *in vitro* mAb release profile in GIT. As expected, a biphasic mAb release was observed for both PLGA-PEG2k and PLGA-PEG5k nanoparticles. However, a higher amount of drug was released from PLGA-PEG5k nanoparticles (25%) in SGF, which could be explained by the higher hydrophilicity of PLGA-PEG5k nanoparticles, which assists in faster release of antibody in the aqueous release media [42]. When drugs are entrapped in a polymer matrix, the release is initiated when water enters the matrix core, where it dissolves and releases the drug. Therefore, a more hydrophilic matrix will allow faster release of the encapsulated drug [43]. The disparity in the amount of mAb released in SGF and FaSSIF can be attributed to the presence of bile salts (a natural surfactant) in FaSSIF which can augment the dissolution process, as discussed previously [40]. Such differences in release pattern in SGF and FaSSIF has been reported previously [26, 44]. This study revealed that the drug release profile is greatly influenced by both; the nature of the nanoparticle and the release media. Overall, the differences in PEG content did not have any influence on the physicochemical properties, drug encapsulation efficiency, and stability. However, the influence was clear in the *in vitro* release studies, where higher PEG content

aided higher burst release of anti-TNF-α antibodies in the gastric medium. As expected, a longer PEG chain length demonstrated a higher PEG content in the nanoparticle. A major proportion of the PEG chain was observed to be present on the surface of the nanoparticles, which demonstrated that the preparation method allowed most of the hydrophilic PEG chains to phase separate and assemble at the nanoparticle surface [45, 46]. Similar outcome was also demonstrated by Xu *et al*, where the emulsification method allowed for more complete partitioning of PEG on the surface of the nanoparticles [23]. The observed minimal interaction of both PLGA-PEG2k and PLGA-PEG5k nanoparticles with mucin solution could be explain by the assembly of PEG chains in dense brush conformation, which has been previously shown to occur when 5-25% PEG content was present [23]. In brief, despite having significantly different PEG content, both the PLGA-PEG nanoparticles exhibited very low interaction with mucin.

The nanoparticles were further evaluated using *in vitro* cell-based studies and *in vivo* DSS-induced acute and chronic colitis models. The cell-based studies were performed to evaluate the cellular toxicity, anti-inflammatory activity, and interaction with intestinal cells. Similar cellular viability results and anti-inflammatory activity were observed for PLGA-PEG2k and PLGA-PEG5k nanoparticles. The confocal images confirmed the ability of the PLGA-PEG nanoparticles to closely interact with the intestinal cell monolayer and be uptaken by the cells, despite different PEG content. A possible reason for these observations could be due to the similar configuration of PEG on the surface of the nanoparticles for both molecular weights, resulting in similar interactions with the cells.

The *in vivo* efficacy of the mAb-loaded nanoparticles was evaluated by assessing the inflammatory response and tissue-associated MPO activity and cytokine level in the acute DSS-colitis murine model. Although no improvement in the weight of animals were observed for all the groups, MPO levels were significantly raised in the DSS-colitis mouse model compared to healthy mice, which was significantly reduced when treated with mAb-PLGA-PEG2k nanoparticles. This is vital as MPO activity is a crucial marker of inflammation in both clinical practice and animal models, especially for the DSS-treated murine model. However, PLGA-PEG5k were not able to demonstrate significant reduction when compared to the control group and PLGA-PEG2k treated group. Quantification of the tissue-associated

TNF- α levels is another crucial parameter when evaluating the anti-inflammatory response. Both, mAb-PLGA-PEG2k and mAb-PLGA-PEG5k nanoparticles significantly reduced the TNF- α levels compared to the control groups, demonstrating efficient drug delivery to the inflamed colonic tissues. These results demonstrate that reduction in the tissue cytokine level is not quite sufficient to observe an overall efficacy in the acute colitis murine model, as observed for mAb-PLGA-PEG5k-treated groups. Overall, the *in vivo* efficacy study demonstrated the mAb-PLGA-PEG2k nanoparticles alleviated inflammation in the colitis model, whereas mAb-PLGA-PEG5k nanoparticles exhibited a lesser pronounced anti-inflammatory response. To further understand discrepancies observed in the *in vivo* study, the nanoparticles' interaction with inflamed colonic epithelia was evaluated *ex vivo.* The *in vivo* results were confirmed where fluorescently-labeled PLGA-PEG2k nanoparticles exhibited higher interaction with inflamed colonic tissues as compared with PLGA-PEG5k nanoparticles. One possible explanation for this outcome could be the higher hydrophilicity of PLGA-PEG5k nanoparticles, which would result in faster degradation of the nanoparticles, and untimely release of the antibody (as observed in the stability study in FeSSIF) [42]. A similar effect on the release pattern of the antibody was also observed in the *in vitro* release studies. Moreover, in the release experiments, a higher amount of antibody was observed to be lost in the gastric conditions from PLGA-PEG5k nanoparticles, thus resulting in a smaller proportion of available antibodies in the intestine. Additionally, the induction of colitis results in alterations in the colonic mucosa, such as epithelial damage, changes in the mucus layer, and colonic milieu. One interesting change in the colonic milieu is the increase in positive charges in the damaged colonic epithelia, due to the accumulation of positively charged molecules such as transferrin and antimicrobial peptides [11, 13, 47, 48]. Therefore, the negatively charged PLGA-PEG2k nanoparticles will have a higher affinity to the positively charged target site as compared to PLGA-PEG5k nanoparticles with a near-neutral charge. The higher binding ability of PLGA-PEG2k nanoparticles was also observed in the *ex vivo* tissue interaction study and could prolong the interaction and augment the accumulation of the released antibody at the target site. Thus, the difference in the surface charge of the nanoparticles could also explain the discrepancies observed in the *in vivo* efficacy studies. The positively charged environment has previously been used as a target site for negatively

charged drug delivery systems [48]. Furthermore, it is also interesting to note that despite observing similar efficacy *in vitro* and in cell-based studies, the *in vivo* response showed PLGA-PEG2k nanoparticles as a superior system for oral anti-TNF-α delivery.

5. Conclusion

In summary, we developed and compared PEGylated PLGA nanoparticles with different surface PEG densities for effective oral delivery of anti-TNF-α. With the use of systematic *in vitro* characterization studies and *in vitro* cell-based screening, we demonstrate the capacity of both PLGA-PEG2k and PLGA-PEG5k nanoparticles to successfully encapsulate the anti-TNF-α mAb. Increasing the PEG chain length resulted in increased surface PEG density, however, both PEG chain lengths were able to display minimal interaction with mucin *in vitro*. The difference in PEG chain length resulted in differences in the *in vitro* release profile and *in vivo* efficacy study, which can be attributed to the higher hydrophilicity of nanoparticles with longer PEG chains. Additionally, in the first attempt to evaluate PLGA-PEG nanoparticles as an efficient oral carrier for anti-TNF-α, we demonstrated the superiority of mAb-PLGA-PEG2k over mAb-PLGA-PEG5k nanoparticles, to effectively exhibit anti-inflammatory responses in an acute murine colitis model. These nanoparticle-based formulations may be adjusted to encapsulate other drugs that could be applied to several disorders at different mucosal surfaces, such as eyes and respiratory tract.

Acknowledgments

N.S. is a postdoctoral researcher from the FRS-FNRS (Fonds de la Recherche Scientifique), Belgium.

REFERENCES

[1] G.G. Kaplan, The global burden of IBD: from 2015 to 2025, Nat. Rev. Gastroenterol. Hepatol. 12 (2015) 720-727.

[2] D. Burger, S. Travis, Conventional medical management of inflammatory bowel disease, Gastroenterol. 140 (2011) 1827-1837.

[3] W. Strober, I.J. Fuss, Proinflammatory cytokines in the pathogenesis of inflammatory bowel diseases, Gastroenterol. 140 (2011) 1756-1767.

[4] B. Khor, A. Gardet, R.J. Xavier, Genetics and pathogenesis of inflammatory bowel disease, Nature. 474 (2011) 307-317.

[5] M. Argollo, G. Fiorino, P. Hindryckx, L. Peyrin-Biroulet, S. Danese, Novel therapeutic targets for inflammatory bowel disease, J. Autoimmun. 85 (2017) 103-116.

[6] M.F. Neurath, Cytokines in inflammatory bowel disease, Nat. Rev. Immunol. 14 (2014) 329-342.

[7] C. Pagnini, T.T. Pizarro, F. Cominelli, Novel Pharmacological Therapy in Inflammatory Bowel Diseases: Beyond Anti-Tumor Necrosis Factor, Front. Pharmacol. 10 (2019) 671-671.

[8] S. de Silva, S. Devlin, R. Panaccione, Optimizing the safety of biologic therapy for IBD, Nat. Rev. Gastroenterol. Hepatol. 7 (2010) 93-101.

[9] A. Stallmach, S. Hagel, T. Bruns, Adverse effects of biologics used for treating IBD, IBD, Best Pract. Res. Clin. Gastroenterol. 24 (2010) A Pediatria167-182.

[10] W. Chan, A. Chen, D. Tiao, C. Selinger, R. Leong, Medication adherence in inflammatory bowel disease, Intest. Res. 15 (2017) 434-445.

[11] S. Hua, E. Marks, J.J. Schneider, S. Keely, Advances in oral nano-delivery systems for colon targeted drug delivery in inflammatory bowel disease: Selective targeting to diseased versus healthy tissue, Nanomedicine. 11 (2015) 1117-1132.

[12] A. Lamprecht, H. Yamamoto, H. Takeuchi, Y. Kawashima, Nanoparticles enhance therapeutic efficiency by selectively increased local drug dose in experimental colitis in rats, J. Pharmacol. Exp. Ther. 315 (2005) 196-202.

[13] B. Tirosh, N. Khatib, Y. Barenholz, A. Nissan, A. Rubinstein, Transferrin as a luminal target for negatively charged liposomes in the inflamed colonic mucosa, Mol. Pharm. 6 (2009) 1083-1091.

[14] L. Sorokin, The impact of the extracellular matrix on inflammation, Nat. Rev. Immunol. 10 (2010) 712-723.

[15] E. Wiener, D. Levanon, Macrophage cultures: an extracellular esterase, Science. 159 (1968) 217.

[16] C. Schmidt, C. Lautenschlaeger, E.M. Collnot, M. Schumann, C. Bojarski, J.D. Schulzke, C.M. Lehr, A. Stallmach, Nano- and microscaled particles for drug targeting to inflamed intestinal mucosa: a first in vivo study in human patients, J. Control. Release. 165 (2013) 139-145.

[17] F. Araujo, N. Shrestha, M.A. Shahbazi, P. Fonte, E.M. Makila, J.J. Salonen, J.T. Hirvonen, P.L. Granja, H.A. Santos, B. Sarmento, The impact of nanoparticles on the mucosal translocation and transport of GLP-1 across the intestinal epithelium, Biomaterials. 35 (2014) 9199-9207.

[18] F. Danhier, E. Ansorena, J.M. Silva, R. Coco, A. Le Breton, V. Preat, PLGA-based nanoparticles: an overview of biomedical applications, J. Control. Release. 161 (2012) 505-522.

[19] L.M. Ensign, C. Schneider, J.S. Suk, R. Cone, J. Hanes, Mucus penetrating nanoparticles: biophysical tool and method of drug and gene delivery, Adv. Mater. 24 (2012) 3887-3894.

[20] S.K. Lai, Y.Y. Wang, J. Hanes, Mucus-penetrating nanoparticles for drug and gene delivery to mucosal tissues, Adv. Drug Del. Rev. 61 (2009) 158-171.

[21] Y. Cu, W.M. Saltzman, Controlled surface modification with poly(ethylene)glycol enhances diffusion of PLGA nanoparticles in human cervical mucus, Mol. Pharm. 6 (2009) 173-181.

[22] C. Lautenschlager, C. Schmidt, C.M. Lehr, D. Fischer, A. Stallmach, PEG-functionalized microparticles selectively target inflamed mucosa in inflammatory bowel disease, Eur. J. Pharm. Biopharm. 85 (2013) 578-586.

[23] Q. Xu, L.M. Ensign, N.J. Boylan, A. Schon, X. Gong, J.C. Yang, N.W. Lamb, S. Cai, T. Yu, E. Freire, J. Hanes, Impact of Surface Polyethylene Glycol (PEG) Density on Biodegradable Nanoparticle Transport in Mucus ex Vivo and Distribution in Vivo, ACS Nano. 9 (2015) 9217-9227.

[24] A. Beloqui, R. Coco, M. Alhouayek, M.A. Solinis, A. Rodriguez-Gascon, G.G. Muccioli, V. Preat, Budesonide-loaded nanostructured lipid carriers reduce inflammation in murine DSS-induced colitis, Int. J. Pharm. 454 (2013) 775-783.

[25] J. Van De Walle, A. Hendrickx, B. Romier, Y. Larondelle, Y.J. Schneider, Inflammatory parameters in Caco-2 cells: effect of stimuli nature, concentration, combination and cell differentiation, Toxicol. In Vitro. 24 (2010) 1441-1449.

[26] N. Shrestha, M.A. Shahbazi, F. Araujo, E. Makila, J. Raula, E.I. Kauppinen, J. Salonen, B. Sarmento, J. Hirvonen, H.A. Santos, Multistage pH-responsive mucoadhesive nanocarriers prepared by aerosol flow reactor technology: A controlled dual protein-drug delivery system, Biomaterials. 68 (2015) 9-20.

[27] S. Wirtz, V. Popp, M. Kindermann, K. Gerlach, B. Weigmann, S. Fichtner-Feigl, M.F. Neurath, Chemically induced mouse models of acute and chronic intestinal inflammation, Nat. Protoc. 12 (2017) 1295-1309.

[28] A. Beloqui, R. Coco, P.B. Memvanga, B. Ucakar, A. des Rieux, V. Preat, pH-sensitive nanoparticles for colonic delivery of curcumin in inflammatory bowel disease, Int. J. Pharm. 473 (2014) 203-212.

[29] S. Melgar, A. Karlsson, E. Michaelsson, Acute colitis induced by dextran sulfate sodium progresses to chronicity in C57BL/6 but not in BALB/c mice: correlation between symptoms and inflammation, Am. J. Physiol. Gastrointest. Liver Physiol. 288 (2005) G1328-1338.

[30] M. Alhouayek, D.M. Lambert, N.M. Delzenne, P.D. Cani, G.G. Muccioli, Increasing endogenous 2-arachidonoylglycerol levels counteracts colitis and related systemic inflammation, The FASEB Journal. 25 (2011) 2711-2721.

[31] A. Garcia-Campos, A.W. Baird, G. Mulcahy, Development of a versatile in vitro method for understanding the migration of Fasciola hepatica newly excysted juveniles, Parasitology. 143 (2016) 24-33.

[32] A.B. Cox, L.A. Rawlinson, A.W. Baird, V. Bzik, D.J. Brayden, In vitro interactions between the oral absorption promoter, sodium caprate (C(10)) and S. typhimurium in rat intestinal ileal mucosae, Pharm. Res. 25 (2008) 114-122.

[33] L.N.M. Ribeiro, V.M. Couto, L.F. Fraceto, E. de Paula, Use of nanoparticle concentration as a tool to understand the structural properties of colloids, Sci. Rep. 8 (2018) 982.

[34] J. Galvez, M. Garrido, M. Merlos, M.I. Torres, A. Zarzuelo, Intestinal anti-inflammatory activity of UR-12746, a novel 5-ASA conjugate, on acute and chronic experimental colitis in the rat, Br. J. Pharmacol. 130 (2000) 1949-1959.

[35] J.E. Krawisz, P. Sharon, W.F. Stenson, Quantitative assay for acute intestinal inflammation based on myeloperoxidase activity. Assessment of inflammation in rat and hamster models, Gastroenterol. 87 (1984) 1344-1350.

[36] M. Naeem, J. Lee, M.A. Oshi, J. Cao, S.P. Hlaing, E. Im, Y. Jung, J.-W. Yoo, Colitis-targeted hybrid nanoparticles-in-microparticles system for the treatment of ulcerative colitis, Acta Biomater. 116 (2020) 368-382.

[37] A.A. Date, G. Halpert, T. Babu, J. Ortiz, P. Kanvinde, P. Dimitrion, J. Narayan, H. Zierden, K. Betageri, O. Musmanno, H. Wiegand, X. Huang, S. Gumber, J. Hanes, L.M. Ensign, Mucus-penetrating budesonide nanosuspension enema for local treatment of inflammatory bowel disease, Biomaterials. 185 (2018) 97-105.

[38] K. Maisel, L. Ensign, M. Reddy, R. Cone, J. Hanes, Effect of surface chemistry on nanoparticle interaction with gastrointestinal mucus and distribution in the gastrointestinal tract following oral and rectal administration in the mouse, J. Control. Release. 197 (2015) 48-57.

[39] K. Maisel, M. Reddy, Q. Xu, S. Chattopadhyay, R. Cone, L.M. Ensign, J. Hanes, Nanoparticles coated with high molecular weight PEG penetrate mucus and provide uniform vaginal and colorectal distribution in vivo, Nanomedicine (Lond.). 11 (2016) 1337-1343.

[40] S. Klein, The Use of Biorelevant Dissolution Media to Forecast the In Vivo Performance of a Drug, The AAPS Journal 12 (2010) 397-406.

[41] N. Shrestha, F. Araújo, M.-A. Shahbazi, E. Mäkilä, M.J. Gomes, B. Herranz-Blanco, R. Lindgren, S. Granroth, E. Kukk, J. Salonen, J. Hirvonen, B. Sarmento, H.A. Santos, Thiolation and Cell-Penetrating Peptide Surface Functionalization of Porous Silicon Nanoparticles for Oral Delivery of Insulin, Adv. Funct. Mater. 26 (2016) 3405-3416.

[42] K. Zhang, X. Tang, J. Zhang, W. Lu, X. Lin, Y. Zhang, B. Tian, H. Yang, H. He, PEG–PLGA copolymers: Their structure and structure-influenced drug delivery applications, J. Control. Release. 183 (2014) 77-86.

[43] A. Beletsi, Z. Panagi, K. Avgoustakis, Biodistribution properties of nanoparticles based on mixtures of PLGA with PLGA-PEG diblock copolymers, Int. J. Pharm. 298 (2005) 233-241.

[44] F. Araujo, N. Shrestha, M.A. Shahbazi, D. Liu, B. Herranz-Blanco, E.M. Makila, J.J. Salonen, J.T. Hirvonen, P.L. Granja, B. Sarmento, H.A. Santos, Microfluidic Assembly of a Multifunctional Tailorable Composite System Designed for Site Specific Combined Oral Delivery of Peptide Drugs, ACS Nano. 9 (2015) 8291-8302.

[45] Q. Xu, N.J. Boylan, S. Cai, B. Miao, H. Patel, J. Hanes, Scalable method to produce biodegradable nanoparticles that rapidly penetrate human mucus, J. Control. Release. 170 (2013) 279-286.

[46] A. Vila, H. Gill, O. McCallion, M.J. Alonso, Transport of PLA-PEG particles across the nasal mucosa: effect of particle size and PEG coating density, J. Control. Release. 98 (2004) 231-244.

[47] H. Monajemi, J. Meenan, R. Lamping, D.O. Obradov, S.A. Radema, P.W. Trown, G.N. Tytgat, S.J. Van Deventer, Inflammatory bowel disease is associated with increased mucosal levels of bactericidal/permeability-increasing protein, Gastroenterol. 110 (1996) 733-739.

[48] S. Zhang, J. Ermann, M.D. Succi, A. Zhou, M.J. Hamilton, B. Cao, J.R. Korzenik, J.N. Glickman, P.K. Vemula, L.H. Glimcher, G. Traverso, R. Langer, J.M. Karp, An inflammation-

targeting hydrogel for local drug delivery in inflammatory bowel disease, Sci. Transl. Med. 7 (2015) 300ra128.

S1. Materials

Copolymers of poly(lactic-co-glycolic acid) and poly(ethylene glycol) (PLGA-PEG, mPEG2k-PLGA10K and mPEG5K-PLGA10K, LA:GA 50:50) were purchased from Nanosoft Biotechnology LLC (NC, USA). Sodium cholate was purchased from Sigma-Aldrich (St. Louis, MO, USA). Anti-TNF-α monoclonal antibody was supplied by UCB Company. The Fab fragment of mAb from murine was stored in 0.1 M phosphate buffer at pH 6.0, and from human was stored in 20 mM sodium acetate buffer at pH 4.5. Sodium chloride was purchased from VWR (Leuven, BE), Sodium monobasic phosphate anhydrous was supplied by Merck (GE), Dichloromethane (DCM) and Sodium hydroxide was provided by Fischer Chemical (UK). Sodium taurocholate, Lecithin, Pepsin and Mucin were purchased from Sigma-Aldrich (St. Louis, MO, USA). Acetonitrile lipopolysachharide (LPS) and Trifluoroacetic acid (gradient HPLC grade) were supplied by VWR chemicals (FR). Ultrapure water was used throughout and obtained from a Milli-Q® Plus apparatus (Millipore). . Deuterated chloroform (CDCl3) and deuterated water (D2O) were supplied by Eurisotop (FR). 3-(trimethylsilyl)-1-propanesulfonic acid sodium salt by was purchased from Merck (GE).

S2. Cell lines and culturing

Caco-2 cells were kindly provided by Dr Maria Rescigno (University of Milano-Bicocca, Milano, Italy) and used from passage x + 25 to x + 30 [1]. Dulbecco's Modified Eagle Medium (DMEM) and Dulbecco's Phosphate-Buffered Saline (PBS) were purchased from Gibco™

Invitrogen Corporation (Paisley, UK). Trypsin (0.05%) with EDTA, non-essential amino-acids (NEAA), L-Glutamine, Penicillin-Streptomycin (10,000 U/mL) and Culture flasks were obtained from Invitrogen (USA). The Caco-2 cell line was maintained medium consisting of DMEM supplemented with 10% (v/v) fetal bovine serum HyClone (FBS), 1% (v/v) L-Glutamine, 1% (v/v) non-essential amino acid (NEAA) and 1% (v/v) antibiotic-antimitotic mixture (Penicillin-Streptomycin). Cells were grown in 75cm² flasks (Corning, Lowell, MA, USA) at 37ºC and in an atmosphere of 10% CO_2/90% air (v/v). The medium for the cell lines were replaced every other day.

J774 murine macrophages were kindly donated by Prof. M.-P. Mingeot (UCL, LDRI, BE) and were maintained in DMEM with 10% (v/v) fetal bovine serum HyClone (FBS). Cells were grown in 75cm2 flasks (Corning, Lowell, MA, USA) at 37ºC and in an atmosphere of 5% CO2/95% air (v/v).

S3. Simulated gastrointestinal fluid

Simulated gastric fluid was composed of 0.2% (w/v) sodium chloride in 0.7% (v/v) hydrochloric acid with 3.2 mg/mL pepsin, with the pH maintained at 1.2. For preparing fasted state simulated intestinal fluid (FaSSIF) (pH 6.8) and fed state simulated intestinal fluid (FeSSIF) (pH 5), the composition is shown in Table 1 [2].

Table 1. FaSSIF and FeSSIF compositions.

	FaSSIF	**FeSSIF**
Sodium Taurocholate	3 mM	15 mM
Lecithin	0.75 mM	3.75 mM
Sodium monobasic phosphate anhydrous	28.65 mM	-
Acetic Acid	-	144.04
Maleic Acid	-	-
Sodium Hydroxide	8.71 mM	101.02 mM
Sodium Chloride (1)	105.85 mM	58.4

S4. Encapsulation efficiency and loading degree

The encapsulation efficiency (EE) and the drug loading (DL) were calculated according to the equation (1) and (2), respectively.

$$EE\ (\%) = \frac{Total\ Drug\ Content\ (\mu g)\ - Unencapsulated\ drug\ amount(\mu g)}{Initial\ drug\ amount\ (\mu g)} \times 100 \qquad Eq(1)$$

$$DL\ (\mu g/mg) = \frac{Total\ Drug\ Content\ (\mu g) - Unencapsulated\ drug\ amount\ (\mu g)}{Total\ solid\ content\ of\ nanoparticles\ (mg)} \qquad Eq(2)$$

S5. High performance liquid chromatography (HPLC) quantification technique

A reversed-phase high performance liquid chromatographic (HPLC) method has been developed and validated for the determination of. An Aeris WIDEPORE 3.6u XB-C8 column (150 x 4.6 mm) (Phenomenex, USA) was used at 80°C in a Shimadzu HPLC (Shimadzu, Japan). Water and acetonitrile were used as mobile phase with 0.05% (v/v) trifluoroacetic acid. A gradient system was developed.

Anti-TNF-α antibody (mAb) was quantified using a gradient method using a Shimadzu HPLC (Shimadzu, Japan). An Aeris WIDEPORE 3.6u XB-C8 column (150 x 4.6 mm) (Phenomenex, USA) was used at 80 °C. The aqueous mobile phase comprised of 0.05% (v/v) trifluoroacetic acid (TFA) in water and the organic mobile phase consisted of 0.05% (v/v) in acetonitrile. A gradient system was developed with an initial ratio of 95:5 (v/v, aqueous: organic phase) at flow rate of 1 mL/min, which was linearly changed to 5:95 (v/v) over 10 min, and kept constant for the next minute. Then, the ratio was linearly changed to initial composition in the next minute and was stabilized for the last three minutes. The injection volume used was 10 µL and the detection wavelength used was 214 nm. The retention time for mAb was 5.6 min. The limit of detection and limit of quantification for anti-TNF-α was 1.1 ± 0.4 µg/mL and 3.3 ± 1.1 µg/mL, respectively.

S6. PEG quantification using ^{1}H NMR

^{1}H NMR spectra were recorded at 400 MHz with relaxation time set at 10 s and ZG at 90°, and number of scans set to 8. To measure the surface PEG content, 3-(trimethylsilyl)-1-propanesulfonic acid, sodium salt (1 wt.-%) was used as an internal standard. A standard calibration curve was prepared for PEG2k and PEG5k homopolymer, with 1% 3-(trimethylsilyl)-1-propanesulfonic acid, sodium salt and deuterated water (D20), which was

used to quantify the PEG content on the surface of the nanoparticles. The actual mass of the nanoparticles was determined by weighing lyophilized nanoparticles. The total PEG content was determined by dissolving the lyophilized nanoparticles in Deuterated chloroform (CDCL3), with hexadeuterodimethyl sulfoxide (1 wt.-%, TMS) as an internal standard. A standard calibration curve was prepared for PEG2k and PEG5k homopolymer, with 1% TMS in CDCL3, which was used to quantify the total PEG content in the nanoparticles. The integration of the peaks in the spectra were done based on the internal standard peak. A representative 1HNMR spectra of PLGA-PEG2k and PLGA-PEG5k nanoparticles in D_2O and CDCl3 is demonstrated in Figure S6. For samples in D_2O with 1 wt% DSS as internal standard, integration of PEG peaks at 3.7 ppm was normalized to the peak at 2.91, 1.76, 0.65 ppm set at 2.0. For samples in D_2O with 1 wt% DSS as internal standard, integration of PEG peaks at 3.7 ppm was normalized to the peak at 0 ppm set at 12. The standard calibration curve prepared for both PEG2k and PEG5k are shown in Figure S7.

For standard calibration curve, PEG2k and PEG5k homopolymer, with 1% 3-(trimethylsilyl)-1-propanesulfonic acid, sodium salt and deuterated water (D2O), was used to quantify the PEG content on the surface of the nanoparticles. The actual mass of the nanoparticles was determined by weighing lyophilized nanoparticles. The total PEG content was determined by dissolving the lyophilized nanoparticles in Deuterated chloroform (CDCl3), with hexadeuterodimethyl sulfoxide (1 wt.-%, TMS) as calibration reference. A standard calibration curve was prepared for PEG2k and PEG5k homopolymer, with 1% TMS in CDCl3, which was used to quantify the total PEG content in the nanoparticles. The standard calibration curve for both homopolymer is shown in Figure S7. The surface and total PEG content were calculated using equation described below:

Surface PEG quantification

$$Surface\ PEG\ content\ (\%) = \frac{Amount\ of\ PEG\ on\ surface\ (\mu g)}{Total\ weight\ of\ nanoparticles\ (\mu g)} \times 100$$

Total PEG quantification

$$Total\ PEG\ content\ (\%) = \frac{Total\ amount\ of\ PEG\ (\mu g)}{Total\ weight\ of\ nanoparticles\ (\mu g)} \times 100$$

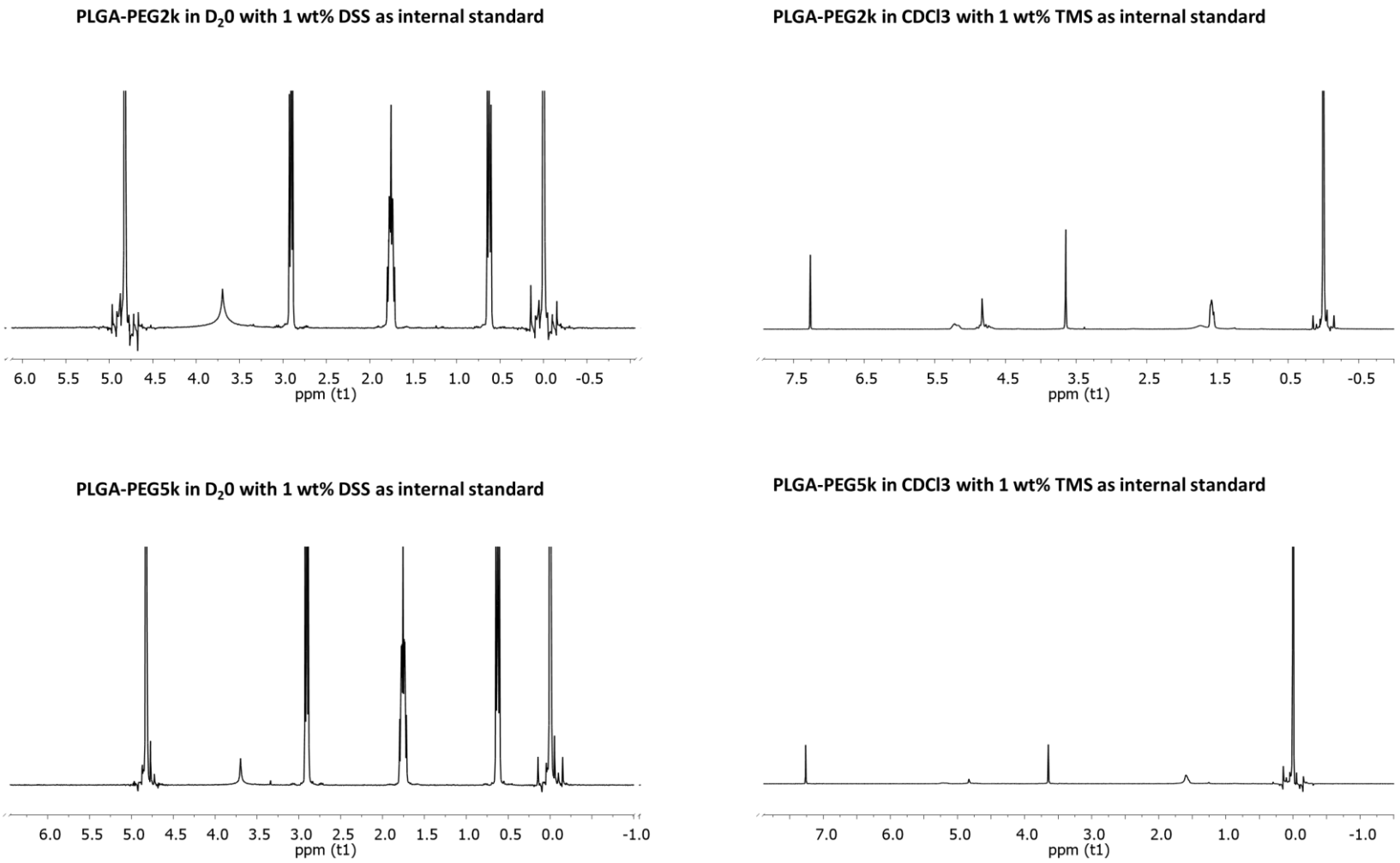

Figure S6a. ^{1}H NMR spectra of PLGA-PEG2k and PLGA-PEG5k in D_2O with 1wt% 3-(trimethylsilyl)-1-propanesulfonic acid, sodium salt as internal standard, and in CDCl3 with 1wt% TMS as internal standard. PEG on nanoparticle shows broadened peak around approx. 3.7 ppm. Peaks at 2.91, 1.76, 0.65 and 0 ppm are from 3-(trimethylsilyl)-1-propanesulfonic acid, sodium salt, and at 0 ppm are for TMS in respective images.

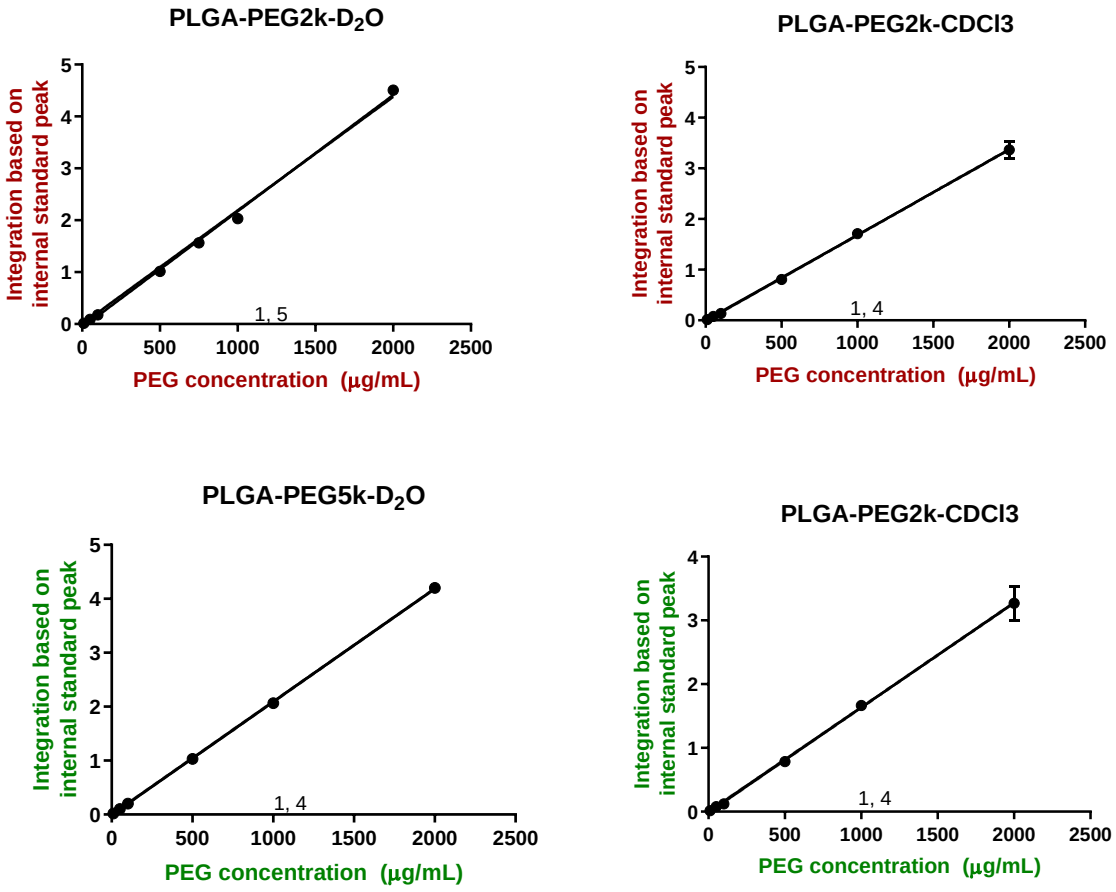

Figure S6b. Calibration curve for the determination of PEG2K and PEG5K in PLGA-PEG2K and PLGA-PEG5K nanoparticles, respectively. To determine surface PEG, calibration curve was constructed in D20, whereas for total PEG content, calibration curve was prepared in CDCL3. (n=3).

S7. Caco-2 cell monolayer

The in vitro intestinal cell monolayer models were formed by seeding 5 x 10^5 Caco-2 cells/well on Transwell® membrane inserts (3 µm pore size) (Corning Costar, Cambridge, U.K.). The cells were cultured for 19-21 days (10% CO_2, 37 °C), with medium replaced in alternate days. Prior to experiments, the integrity of the monolayer was evaluated by measuring the trans-epithelial electrical resistance (TEER) using an epithelial voltohm meter (EVOM, World Precision Instruments, Berlin, DE). The monolayers with TEER values over 400 Ω cm^2 were used.

S8. In vivo efficacy study in chronic colitis model

For the chronic colitis model, the inflammation was induced by administration of 2.5% dextran sulfate sodium (DSS) in drinking water for one week, followed by two weeks of washout period. A total of

three cycles of DSS were administered to mice (Week 1, 4 and 7) [3].. The inflammatory readouts were finally assessed on day 50. The schematic representation of the chronic study is shown in figure below. Four groups were created with 10 animals in each group: (i) Untreated healthy control group; (ii) DSS treated control group; (iii) antibody-loaded PLGA-PEG2K nanoparticles treated group (200 mg/kg of nanoparticles), and (iv) antibody-loaded PLGA-PEG5K nanoparticles treated group (200 mg/kg of nanoparticles). The nanoparticles were administered via oral gavage, and for control groups water was administered via the same method. The gavage was performed every day from week 7 until week 9. The weights of mice were assessed every day until the end of the experiment. On day 50, the animals were sacrificed, and colon tissue samples were collected for further analysis. Similar to acute study, the samples were evaluated based on clinical activity scoring, colon weight/length ratio, myeloperoxidase activity, tissue cytokine quantification and histological assessment. The details of the methods are already described in detail in the main file (section 2.7 in main file).

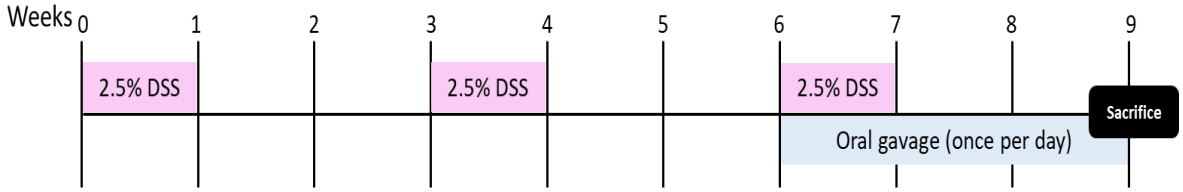

Figure S8: Schematic representation of the chronic in vivo model used and the experiment schedule.

S9. Acute colitis model

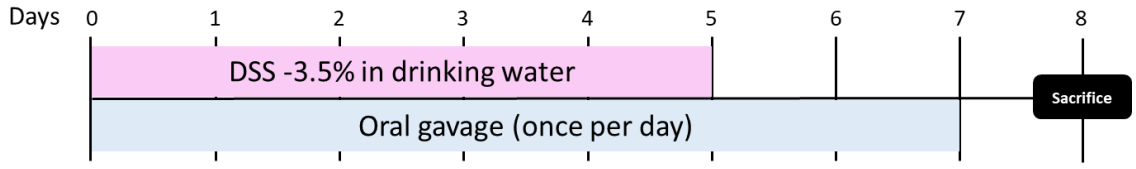

Figure S9: Schematic representation of acute colitis model induction and the experimental plan

S10. Ex vivo Eppendorf chamber model

The Eppendorf chamber method is a modified version of horizontal diffusion chamber [4]. The chamber comprises of apical and basolateral compartments. The basolateral chamber is a beaker with 50 mL of Krebs-Henseleit buffer (composition shown in Table 2) with continuous supply of carbogen gas. The apical chamber was comprised of a 500 µL Eppendorf tube with the tapered end removed using a razor blade. The lid was detached and a holedrilled through the centre to create a space where

the tissue section was placed, and from where the tissue was in the intersection of apical and basolateral chambers (as shown in Figure below). The entire set-up was placed in a water bath, to maintain the temperature of 37 °C throughout the study.

The chamber comprises of apical and basolateral compartments The basolateral chamber is a beaker with 50 mL buffer with continuous supply of carbogen gas. The apical chamber used was a 500 µL of Eppendorf tube with the lid drilled to create a space where the tissue section is placed, and from where the tissue is in the intersection of apical and basolateral chambers (as shown in the Figure below). The entire setting was placed in a water bath, to maintain the temperature of 37 °C throughout the study.

Table 2: Composition of Krebs-Henseleit buffer

Composition	**Amount for 100 mL buffer**
$MgSO_4$-$7H_2O$	2.96 g
KH_2PO_4	1.63 g
$CaCl_2$	3.68 g
KCl	3.5 g
NaCl	0.658 g
$NaHCO_3$	0.21 g
D-Glucose	0.216 g

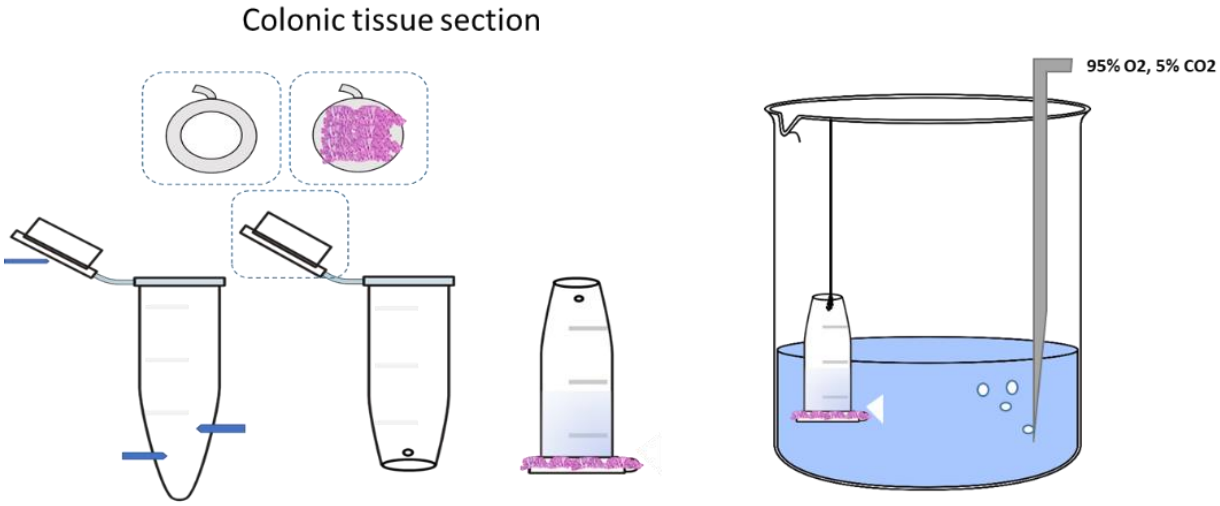

Figure S10: Schematic representation of Eppendorf chamber model for ex vivo study.

S11. Stability of nanoparticles

The stability of PLGA-PEG2K and PLGA-PEG5K nanoparticles was studied in simulated gastrointestinal fluids: SGF, FaSSIF and FeSSIF. Both PLGA-PEG2K and PLGA-PEG5K nanoparticles demonstrated stability in SGF and FaSSIF by retaining their polydispersity index, as shown in Figure, S11.

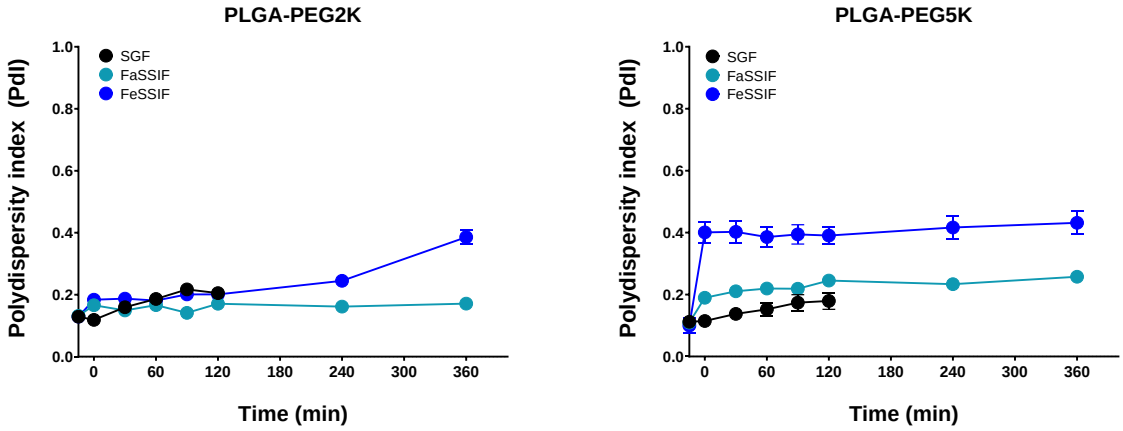

Figure S11. The in vitro stability study of PLGA-PEG2K and PLGA-PEG5K nanoparticles in simulated gastric fluid (SGF), Fasted state simulated intestinal fluid (FaSSIF), and fed state simulated intestinal fluid (FeSSIF). The polydispersity index of the nanoparticles was measured using dynamic light scattering.

S12. In vivo efficacy study of mAb solution in DSS induced acute colitis murine model

The experiment demonstrated that the mAb solution did not show any effect on the acute colitis mice model. No significant improvement in the weight of the animals was observed when treated with the mAb solution (Figure 12A). Furthermore, there was no improvement observed in terms of weigh/length ratio of the colon for mAb treated group as compared to DSS control group (Figure 12B). When analyzing the TNF-α expression in the colonic tissue (Figure 12C), no significant reduction in the protein expression of the TNF-α was observed for mAb treated group. Similarly, the histological images exhibited similar result where signs of inflammation were observed for mAb treated mice colon (Figure 12D). Therefore, in our current study we did not use the drug solution as a control group in an attempt to minimize the use of animals in the experiment.

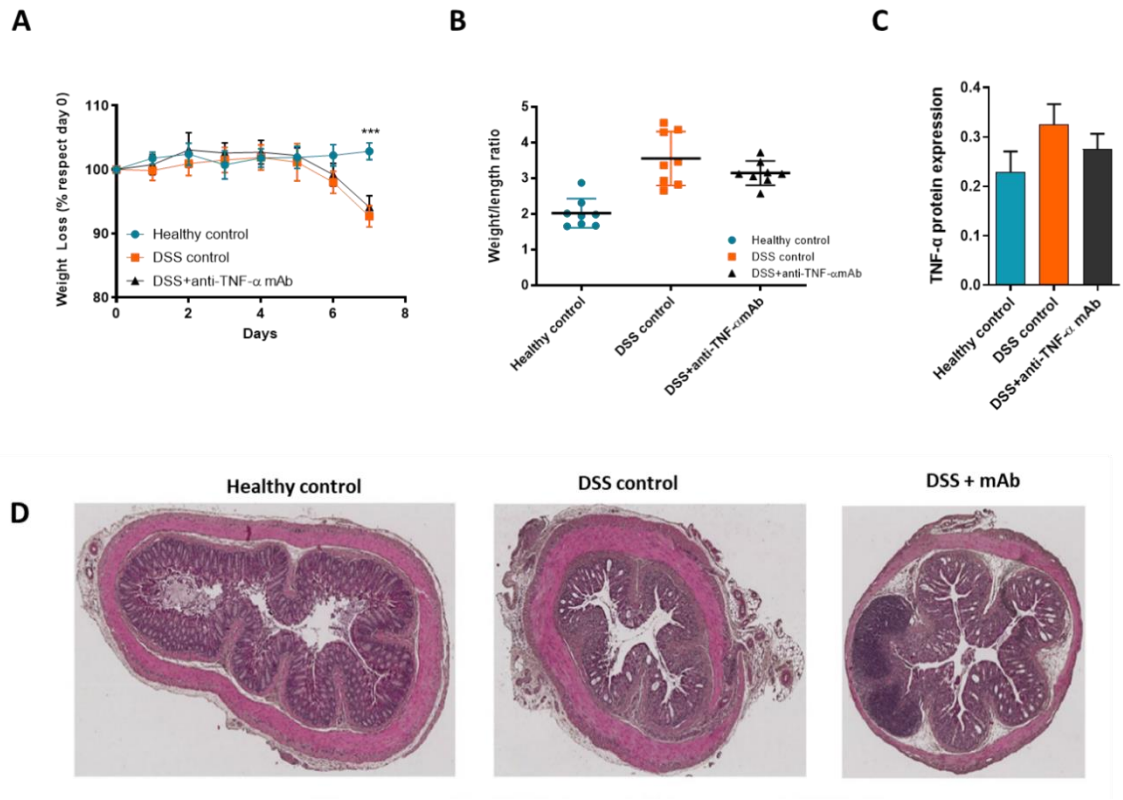

Figure 12 In vivo efficacy study of mAb solution in DSS induced acute colitis murine model. The study included three groups (with eight mice in each group): (i) healthy mice, (ii) DSS treated control mice, (iii) mAb treated DSS mice. (A) Daily changes in body weight in DSS-induced acute colitis mice and in healthy mice (% respect to initial weight at day 1). (B) Colon weight/length ratio for all the tested groups. (C) TNF-α protein expressions in colonic tissues on day 8 (D) Histological sections of the colon stained with hematoxylin-eosin. Data shown as mean ± SEM (n=6) (*** p< 0.001 as compared to DSS treated control group)

S13 Histology in acute colitis model

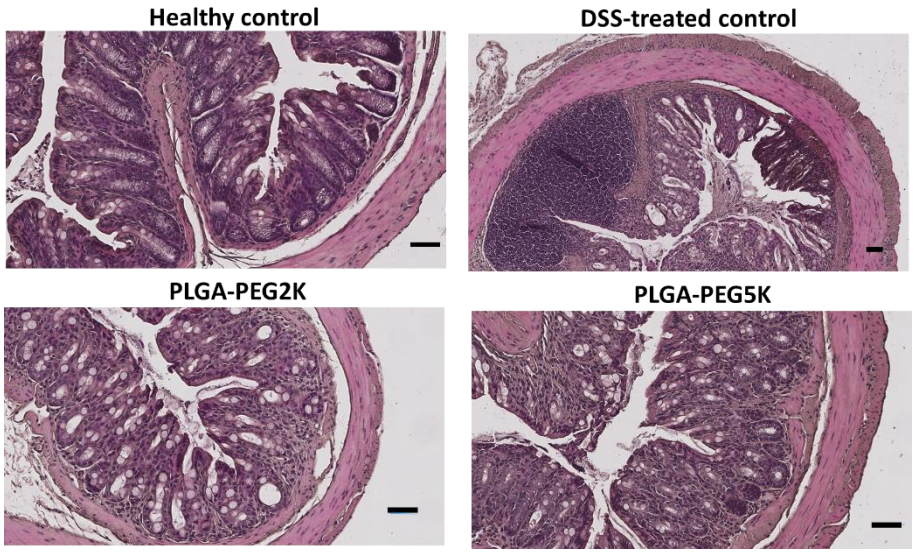

Figure S13. Histological sections of the colon stained with hematoxylin-eosin (Scale bar = 50 µm).

S14. In vivo efficacy in chronic colitis model

The DSS colitis murine model was induced as described in S8. However, from Figure S13, it can be clearly observed that the animals recovered on their own after the third DSS treatment, with or without treatment with mAb loaded nanoparticles. Despite of some changes observed in colon weight/length, the lack of sufficient inflammation in the murine model was further confirmed by very low levels of MPO activity and TNF-α level in the colonic tissues. It can be seen that MPO activity in the colitis induced colonic tissues is similar to healthy colonic tissues. Moreover, the levels of TNF-α in the colonic tissues was ten-fold lower than that observed in the acute model. Due to inability to establish chronic colitis in the murine model, the in vivo efficacy of the nanoparticles was not successfully evaluated. For future studies, a different chronic colitis model should be used to further confirm the efficacy of these nanoparticles.

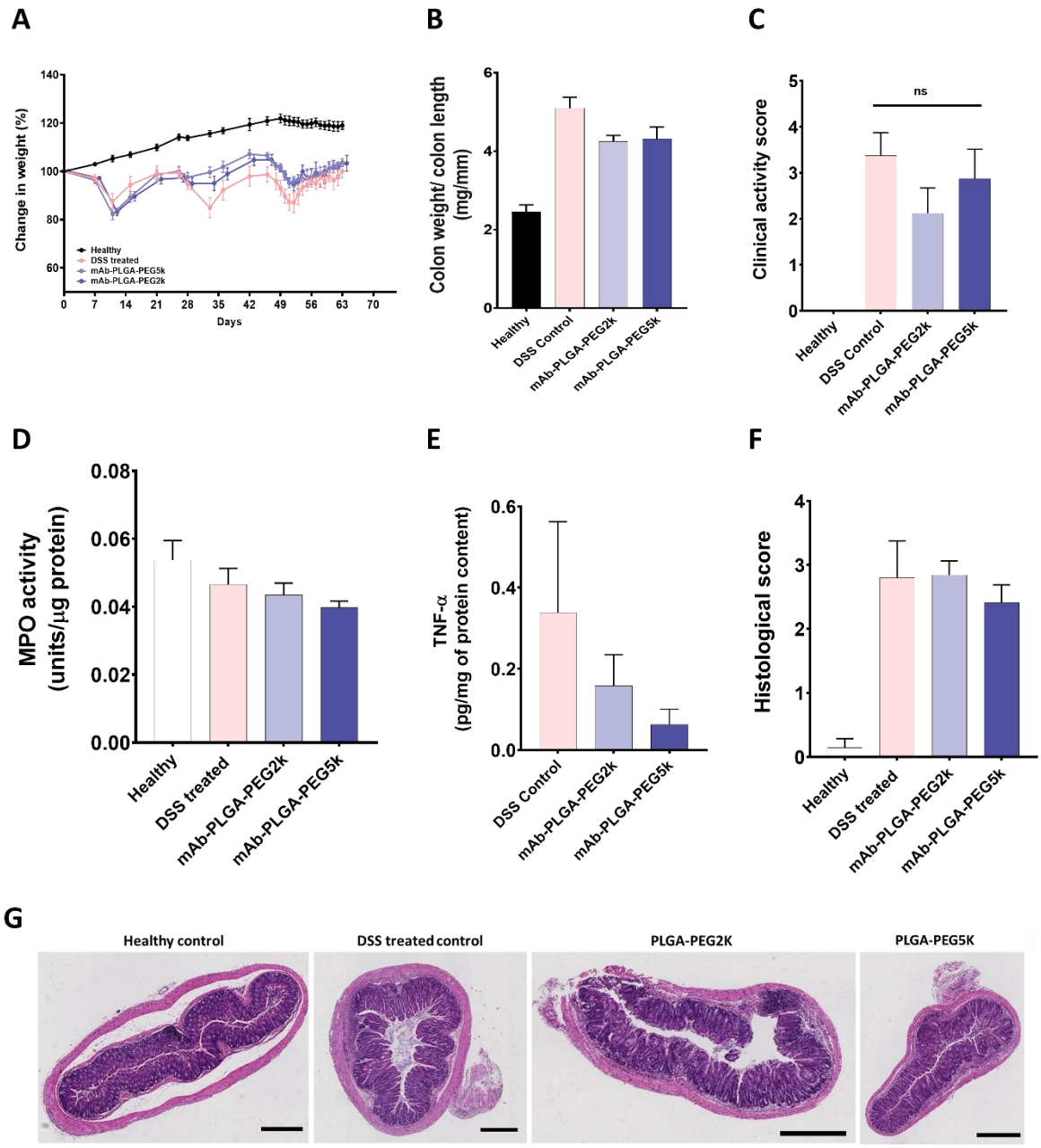

Figure S14. In vivo efficacy study in DSS induced chronic colitis murine model. The study included four groups (with eight mice in each group): (i) healthy mice, (ii) DSS treated control mice, (iii) PLGA-PEG2K treated DSS mice, and (iv) PLGA-PEG5K treated DSS mice. (A) Daily changes in body weight in DSS-induced acute colitis mice and in healthy mice (% respect to initial weight at day 1). (B)) Colon weight/length ratio for all the tested groups. (C) MPO activity and (D) pro-cytokine TNF-α levels in colonic tissues on day 8 (E) Blind histological scoring of the colonic tissues of the groups and (F) Histological sections of the colon stained with hematoxylin-eosin (Scale bar = 400 μm). Data shown as mean ± SEM (n=8).

References

1. Rescigno, Maria, Gianluca Rotta, Barbara Valzasina, and Paola Ricciardi-Castagnoli. "Dendritic cells shuttle microbes across gut epithelial monolayers." Immunobiology 204, no. 5 (2001): 572-581.

2. Roger, Emilie, Frédéric Lagarce, and J-P. Benoit. "The gastrointestinal stability of lipid nanocapsules." International journal of pharmaceutics 379, no. 2 (2009): 260-265.

3. Wirtz, Stefan, Vanessa Popp, Markus Kindermann, Katharina Gerlach, Benno Weigmann, Stefan Fichtner-Feigl, and Markus F. Neurath. "Chemically induced mouse models of acute and chronic intestinal inflammation." Nature protocols 12, no. 7 (2017): 1295.

4. Soni, Jyoti, Alan W. Baird, Leah M. O'Brien, Maire McElroy, John J. Callanan, Hugh F. Bassett, Deirdre Campion, and David J. Brayden. "Rat, ovine and bovine Peyer's patches mounted in horizontal diffusion chambers display sampling function." Journal of controlled release 115, no. 1 (2006): 68-77.